(12) INTERNATIONAL APPLICATION PUBLISHED UNDER THE PATENT COOPERATION TREATY (PCT)

(19) World Intellectual Property Organization
International Bureau

(43) International Publication Date
24 December 2008 (24.12.2008)

PCT

(10) International Publication Number
WO 2008/157680 A2

(51) International Patent Classification:
G06F 19/00 (2006.01)

(21) International Application Number:
PCT/US2008/067477

(22) International Filing Date: 19 June 2008 (19.06.2008)

(25) Filing Language: English

(26) Publication Language: English

(30) Priority Data:
60/945,404 21 June 2007 (21.06.2007) US

(71) Applicants *(for all designated States except US)*: **THE WISTAR INSTITUTE** [US/US]; 3601 Spruce Street, Philadelphia, PA 19104-4268 (US). **THE JOHNS HOPKINS UNIVERSITY** [US/US]; 3400 North Charles Street, Baltimore, MD 21218 (US).

(72) Inventors; and

(75) Inventors/Applicants *(for US only)*: **MARMORSTEIN, Ronen** [US/US]; 31 College Avenue, Swarthmore, PA 19081-1424 (US). **LIU, Xin** [CN/US]; 418 S. 44th Street, Apartment B7, Philadelphia, PA 19104 (US). **COLE, Philip, A.** [US/US]; 16 Hambleton Court, Baltimore, MD 21205 (US). **WANG, Ling** [CN/US]; 12030 12th Avenue Ne, Apartment 409d, Seattle, WA 98125 (US). **BOWERS, Erin, M.** [US/US]; 3133 Tilden Drive, Baltimore, MD 21211 (US). **MEYERS, David, J.** [US/US]; 623 Lake Drive, Towson, MD 21286 (US). **MUKHERJEE, Chandrani** [IN/US]; 3120 Saint Paul Street, Baltimore, MD 21218 (US).

(74) Agents: **LICATA, Jane, Massey** et al.; Licata & Tyrrell P.c., 66 E. Main Street, Marlton, NJ 08053 (US).

(81) Designated States *(unless otherwise indicated, for every kind of national protection available)*: AE, AG, AL, AM, AO, AT, AU, AZ, BA, BB, BG, BH, BR, BW, BY, BZ, CA, CH, CN, CO, CR, CU, CZ, DE, DK, DM, DO, DZ, EC, EE, EG, ES, FI, GB, GD, GE, GH, GM, GT, HN, HR, HU, ID, IL, IN, IS, JP, KE, KG, KM, KN, KP, KR, KZ, LA, LC, LK, LR, LS, LT, LU, LY, MA, MD, ME, MG, MK, MN, MW, MX, MY, MZ, NA, NG, NI, NO, NZ, OM, PG, PH, PL, PT, RO, RS, RU, SC, SD, SE, SG, SK, SL, SM, SV, SY, TJ, TM, TN, TR, TT, TZ, UA, UG, US, UZ, VC, VN, ZA, ZM, ZW.

(84) Designated States *(unless otherwise indicated, for every kind of regional protection available)*: ARIPO (BW, GH, GM, KE, LS, MW, MZ, NA, SD, SL, SZ, TZ, UG, ZM, ZW), Eurasian (AM, AZ, BY, KG, KZ, MD, RU, TJ, TM),

[Continued on next page]

(54) Title: METHODS AND COMPOSITIONS FOR MODULATING P300/CBP ACTIVITY

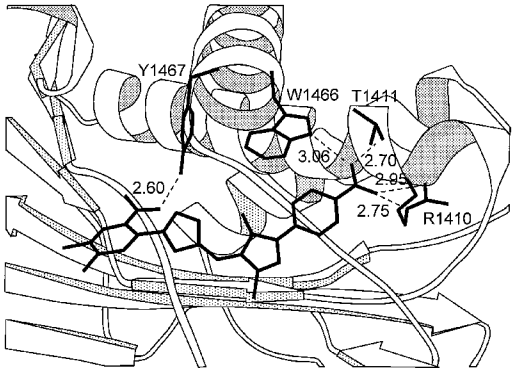

FIG. 11

(57) Abstract: The present invention relates to a method for identifying compounds that modulate the activity of p300/CBP. Compounds of the invention are identified by designing or screening for a compound which binds to at least one amino acid residue of the newly identified lysine-CoA inhibitor binding site, L1loop, electronegative pocket, or electronegative groove of the HAT domain of p300/CBP and testing the compound for its ability to modulate the activity of p300/CBP. Compositions and methods for preventing or treating diseases or disorders associated with p300/CBP are also provided as is a method for producing a semi -synthetic HAT domain.

WO 2008/157680 A2

European (AT, BE, BG, CH, CY, CZ, DE, DK, EE, ES, FI, FR, GB, GR, HR, HU, IE, IS, IT, LT, LU, LV, MC, MT, NL, NO, PL, PT, RO, SE, SI, SK, TR), OAPI (BF, BJ, CF, CG, CI, CM, GA, GN, GQ, GW, ML, MR, NE, SN, TD, TG).

Published:

— *without international search report and to be republished upon receipt of that report*

— *with sequence listing part of description published separately in electronic form and available upon request from the International Bureau*

METHODS AND COMPOSITIONS FOR MODULATING P300/CBP ACTIVITY

Introduction

This application claims benefit of priority to U.S. Provisional Patent Application Serial No. 60/945,404, filed June 21, 2007, the content of which is incorporated herein by reference in its entirety.

This invention was made with government support under grant Nos. GM060293 and GM062437 awarded by the National Institutes of Health. The government has certain rights in the invention.

Background of the Invention

The CBP and p300 paralogs were identified by their roles in regulating cyclic AMP-related gene activation and binding to adenoviral protein E1A, respectively (Chrivia, et al. (1993) *Nature* 365:855-859; Eckner, et al. (1994) *Genes Dev.* 8:869-884). One or more copies of the p300/CBP transcriptional coactivator is encoded in organisms from worm to man, and they have been intensively studied because of their diverse and important roles in complex biological processes (Goodman & Smolik (2000) *Genes Dev.* 14:1553-1577). The p300/CBP protein is ~250 kDa and contains a number of well-defined domains, many of which are crucial for its recruitment by a wide range of transcription factors (Legge, et al. (2004) *J. Mol. Biol.* 343:1081-1093; Mujtaba, et al. (2004) *Mol. Cell* 13:251-263; Radhakrishnan, et al. (1997) *Cell* 91:741-752). p300/CBP has been shown to possess intrinsic histone acetyltransferase (HAT) activity which has led to a wide array of insights into its biological activities (Bannister & Kouzarides (1996) *Nature* 384:641-643; Ogryzko, et al. (1996) *Cell* 87:953-959). For example, p300/CBP HAT activity is important for its ability

to act as a coactivator for a variety of transcription factors, *e.g.*, p53, NFκB, STAT3, GATA-1, MyoD, TCF, androgen receptor (AR), and HIV Tat; thereby indicating that its HAT activity is important for a variety of pathways including cancer (Iyer, et al. (2004b) *Oncogene* 23:4225-4231), HIV (Kaehlcke, et al. (2003) *Mol. Cell* 12:167-176) and HTLV-1 (Georges, et al. (2003) *Mol. Cell Biol.* 23:3392-3404) pathogenesis; as well as, cardiac remodeling (Gusterson, et al. (2003) *J. Biol. Chem.* 278:6838-6847), glucose regulation (van der Heide & Smidt (2005) *Trends Biochem. Sci.* 30:81-86), oxygen sensing (Roe, et al. (2006) *Mol. Cell* 22:395-405), and steroid hormone signaling (Korzus, et al. (1998) *Science* 279:703-707). In addition to catalyzing the acetylation of multiple lysines on all four core histones, p300/CBP has been shown to acetylate a wide array of transcription factors and other proteins as part of its functions. Some of these p300/CBP-acetylated substrates include p53, p73, NFκB, STAT3, GATA-1, MyoD, TCF, E2F1, HMG14, HMGI(Y), androgen receptor (AR), Tat, and c-Myb (Chen, et al. (2001) *Science* 293:1653-1657; Costanzo, et al. (2002) *Mol. Cell* 9:175-186; Thompson, et al. (2001) *J. Biol. Chem.* 276:33721-33729; Yuan, et al. (2005) *Science* 307:269-273). Although there are no precise consensus sequences for p300/CBP-mediated acetylation, there is a clear preference for nearby positively charged residues influencing targeted lysine acetylation (Thompson, et al. (2001) *supra*).

As noted above, p300/CBP plays a key role in regulating the transcription of a large subset of eukaryotic genes. Consistent with this important role is the fact that mutations, altered expression, and gene rearrangements of p300/CBP have been observed in a variety of diseases including cancer (Iyer, et al. (2004b) *supra*).

For example, patients with Rubinstein-Taybi Syndrome, which involves a heterozygous mutation in one CBP allele (Murata, et al. (2001) *Hum. Mol. Genet.* 10:1071-1076), have an increased incidence of tumors. Additionally, point mutations thought to interfere with the catalytic activity of p300/CBP have been observed in pancreatic cancer (Gayther, et al. (2000) *Nat. Genet.* 24:300-303), colon cancer (Muraoka, et al. (1996) *Oncogene* 12:1565-1569), and lung cancer (Kishimoto, et al. (2005) *Clin. Cancer Res.* 11:512-519). Gene fusion events involving the CBP HAT domain have been detected in a number of acute leukemias (Borrow, et al. (1996) *Nat. Genet.* 14:33-41). Finally, overexpression of p300/CBP has been detected in a variety of cancers including colon (Pena, et al. (2006) *Int. J. Cancer* 119:2098-2104), gastric (Kim, et al. (2007) *Am. J. Physiol. Cell Physiol.* 292:C857-866), and thyroid (Fluge, et al. (2006) *Thyroid* 16:161-175) carcinoma.

The coactivator activity of p300/CBP is controlled at multiple levels and its regulation has been studied (Goodman & Smolik (2000) *supra*). For example, p300/CBP is known to be phosphorylated, methylated, ubiquitinated, sumoylated, and acetylated and these modifications exert a myriad of effects on p300/CBP coactivator activity by modulating its protein levels, its interactions with other proteins, and its HAT activity (Goodman & Smolik (2000) *supra*; Thompson, et al. (2004) *Nat. Struct. Mol. Biol.* 11:308-315). Regarding acetylation, there are a dense cluster of lysines in a flexible loop region of the p300/CBP HAT domain that are sites of autoacetylation (Thompson, et al. (2004) *supra*). Intermolecular autoacetylation of these lysines appears to upregulate p300/CBP HAT activity (Thompson, et al. (2004) *supra*) and also modulate protein-protein interactions with APC

(Turnell, et al. (2005) *Nature* 438:690-695), PIC (Black, et al. (2006) *Mol. Cell* 23:809-818), and ATF-2 among possibly others. Partial deletion of this p300/CBP autoacetylated loop can upregulate HAT activity and modulate transcriptional activation (Thompson, et al. (2004) *supra*).

Studies investigating the structure, mechanism, and inhibition of different HATs have been conducted. The most well-understood HATs are the paralogs PCAF and GCN5, and these enzymes appear to be classical members of the GNAT superfamily (Neuwald & Landsman (1997) *Trends Biochem. Sci.* 22:154-155) based on structure and catalytic mechanism (Vetting, et al. (2005) *Arch. Biochem. Biophys.* 433:212-226). The GNAT superfamily is composed of weakly conserved acetyltransferases with ~200 residue catalytic domains that show a similar core protein fold and include enzymes involved in antibiotic resistance, melatonin biosynthesis, and polyamine metabolism (Vetting, et al. (2005) *supra*). The catalytic mechanism of PCAF/GCN5 and most other GNATs usually involves a ternary complex mechanism with ordered binding of the acetyl-CoA substrate prior to the amine substrate (Vetting, et al. (2005) *supra*). Upon ternary complex formation, there is direct transfer of the acetyl group from acetyl-CoA to the substrate amino group. The α-β fold for acetyl-CoA binding is quite conserved and many of these enzymes appear to have a catalytic base assisting in amine substrate deprotonation (Vetting, et al. (2005) *supra*). Bisubstrate analog inhibitors in which the amine substrate are linked to coenzyme A via an acetyl bridge have proved to be powerful inhibitors for these enzymes and have been extensively used in biochemical and structural studies (Vetting, et al. (2005) *supra*).

Sequence alignments and enzymology experiments on p300/CBP have led to somewhat confusing and contradictory

results regarding the mechanism of p300/CBP and its structural relationship to PCAF/GCN5. For example, sequence alignments of p300/CBP and PCAF/GCN5 (Martinez-Balbas, et al. (1998) *EMBO J.* 17:2886-2893; Yuan & Giordano (2002) *Oncogene* 21:2253-2260) have shown limited homology that appears to be inconsistent with the PCAF/GCN5 structure (Poux, et al. (2002) *Proc. Natl. Acad. Sci. USA* 99:14065-14070). Additionally, a two substrate kinetic analysis showed a parallel line pattern suggestive of a ping-pong kinetic mechanism with a covalent enzyme intermediate (Thompson, et al. (2001) *supra*), potentially similar to the mechanism employed by Esa1 (Berndsen, et al. (2007) *Biochemistry* 46:623-629) and different from PCAF/Gcn5 (Tanner, et al. (1999) *J. Biol. Chem.* 274:18157-18160; Trievel, et al. (1999) *Proc. Natl. Acad. Sci. USA* 96:8931-8936; Vetting, et al. (2005) *supra*). However, experiments with acetyl-CoA-based affinity labeling agents failed to identify a key active site nucleophilic residue that would play a role in forming a covalent intermediate. Interestingly, the nominal bisubstrate analog Lys-CoA in which a derivatized lysine is bridged to coenzyme A via an acetyl linker is a powerful and selective inhibitor of p300/CBP (Lau, et al. (2000) *Mol. Cell* 5:589-595). Paradoxically, longer peptide-CoA conjugates, based on better peptide substrates of p300 HAT, are weaker p300 HAT inhibitors (Lau, et al. (2000) *supra*). This pattern is reversed for PCAF/GCN5 where longer rather than shorter peptide-CoA conjugates are better HAT **PCA** Compound **F**/GCN5 inhibitors (Lau, et al. (2000) *supra*), consistent with their substrate behaviors and ternary complex mechanisms. Interestingly, deletion of the 3'-phosphate from Lys-CoA results in a 30-fold reduction in p300 HAT inhibitory potency (Cebrat, et al. (2003) *Bioorg. Med. Chem.* 11:3307-

3313). In contrast, for a GNAT superfamily member serotonin N-acetyltransferase bisubstrate analog the 3'-phosphate is essentially completely dispensable (Khalil, et al. (1999) *Proc. Natl. Acad. Sci. USA* 96:12418-12423). Taken together, these studies provide little information of the nature of p300/CBP HAT mechanism and structure.

Summary of the Invention

The present invention is a method for identifying a compound which modulates the activity of p300/CBP. The method of this invention involves, (a) designing or screening for a compound which binds to at least one amino acid residue of the lysine-CoA inhibitor binding site, L1 loop, electronegative pocket, or electronegative groove of the HAT domain of p300/CBP; and (b) testing the compound designed or screened for in (a) for its ability to modulate the activity of p300/CBP, thereby identifying a compound that modulates the activity of p300/CBP. In one embodiment, the compound binds to the substrate binding site and inhibits the activity of p300/CBP. In other embodiments, step (a) is carried out *in silico* or *in vitro*. Compounds identified by the present invention and pharmaceutical compositions containing the same are also provided.

The present invention also provides a method for making an inhibitor of p300/CBP. This method involves screening for a compound which interacts with amino acid residues Arg1410, Thr1411, Trp1466, and Tyr1467 of SEQ ID NO:1 or amino acid residues Arg1446, Thr1447, Trp1502 and Tyr1503 of SEQ ID NO:2 thereby making an inhibitor of p300/CBP.

Methods for inhibiting the activity of p300/CBP and preventing or treating cancer, diabetes, or obesity using

one or more p300/CBP inhibitors of the invention are also provided.

The present invention is also a method for producing a semi-synthetic HAT domain. The method involves subjecting a HAT domain and N-Cys peptide of p300/CBP to expressed protein ligation to produce a semi-synthetic HAT domain; and subjecting the semi-synthetic HAT domain to proteolysis in the presence of an inhibitor thereby producing a heterodimeric HAT complex.

Brief Description of the Drawings

Figure 1 shows the structure of p300 and preparation and structure of p300 HAT domain. Figure 1A is a schematic representation of p300 domain structure with selected interacting proteins. Figure 1B is a scheme of expressed protein ligation strategy for semi-synthetic p300 HAT domain preparation.

Figure 2 shows the relative activity of several mutants around the p300 HAT domain active site as inferred from the structure. The activity was measured using 50 nM enzyme, 20 μM AcCoA and 200 μM H4-15 for most of the mutants. W1436A, H1434A activity was measured using 50 nM enzyme, 200 μM AcCoA and 200 μM H4-15. Sub-saturating concentrations of AcCoA and H4-15 were used to more easily detect the difference between wild-type p300 and mutants resulting from K_m changes. Wild-type (W.T.) p300 activity was measured under each condition to normalize the relative activity of the mutants.

Figure 3 is a schematic view of p300 HAT domain interactions with the Lys-CoA inhibitor. Hydrophobic interactions and hydrogen bonds are indicated with solid and dotted arrows, respectively.

Figure 4 shows the sequence alignments of histone (H2A, SEQ ID NO:3; H2B, SEQ ID NO:4; H3, SEQ ID NO:5; and H4, SEQ ID NO:6) and non-histone (p53, SEQ ID NO:7; p73, SEQ ID NO:8; HMG14, SEQ ID NO:9; E2F1, SEQ ID NO:10; dTCF, SEQ ID NO:11; HMGI(Y), SEQ ID NO:12; ATF-2, SEQ ID NO:13; c-Myb, SEQ ID NO:14; NFκB, SEQ ID NO:15; STAT3, SEQ ID NO:16; mGATA-1, SEQ ID NO:17; MyoD, SEQ ID NO:18; AR, SEQ ID NO:19; Tat, SEQ ID NO:20; p300, SEQ ID NO:21) p300 substrates with all positively charged residues are underlined. The preferred acetylation sites are indicated by the box and the proximal lysine or arginine residues are marked with a star.

Figure 5 depicts the results of a mutagenesis study showing the relative activity of several putative substrate binding mutants. The activity was measure using 50 nM enzyme, 200 μM AcCoA and 200 μM H4-15; and is plotted as activity relative to wild-type (W.T.) p300.

Figure 6 shows the anticipated catalytic mechanism of p300 HAT. Figure 6A is a schematic of the catalytic mechanism of p300/CBP. Figure 6B is a pH-rate profile of wild-type p300. The pka is at 8.36±0.14. The pH-rate profiles of Y1467F, Y1394F and H1434A were also measured and were found to not be significantly different from that of wild-type p300.

Figure 7 depicts the results of a mutagenesis study showing the relative activity of cancer associated mutants. p300 wt and disease mutants for these studies do not contain the internal deletion of residues 1523-1554 used for the structural studies; however, they were allowed to activate by pre-incubation with acetyl-CoA. V/K is the $V_{max}/K_{m\ (H4-15)}$. D1399Y, R1342P steady state assays were carried out using a radioactive assay because of their low

activity with 20 μM AcCoA. All the other mutants were evaluated using a nonradioactive HAT assay with 2 mM AcCoA.

Figure 8 shows the amino acid sequences of human p300 and human CBP. An overall structure and amino acid sequence comparison of the human p300 (SEQ ID NO:22) and human CBP (SEQ ID NO:23) HAT domain are shown.

Figure 9 shows H4-CoA-20 linker variants for structural analysis.

Figure 10 shows the pattern of inhibition of compound **7** versus acetyl-CoA (Figure 10A) or H4-15 (Figure 10B).

Figure 11 shows a docking model of compound **7** bound to p300 HAT. Inhibitor **7** is shown as a stick drawing and enzyme residues interacting with inhibitor **7** are indicated.

Detailed Description of the Invention

The transcriptional coactivator p300/CBP is a histone acetyltransferase (HAT) that regulates gene expression by acetylating histones and other transcription factors and the dysregulation of p300/CBP HAT activity contributes to various diseases including cancer. The p300/CBP proteins contain a number of well-defined domains (Figure 1A), many of which are crucial for recruitment by a wide range of transcription factors. The high-resolution crystal structure of the human p300 HAT domain in complex with a specific bisubstrate analog inhibitor, Lys-CoA, has now been determined. The structure reveals similarity with other HAT domains in the CoA-binding region, despite the lack of sequence conservation within this region, and a novel, and presumably flexible, cofactor-binding loop within the CoA-binding core region that makes additional interactions with cofactor. HAT regions flanking the core CoA binding regions show significant structural divergence with other HATs and appears to help form a unique substrate

recognition region. Structure-guided mutagenesis indicates that p300/CBP uses a different catalytic mechanism than other HATs. Mapping of p300 tumor-derived mutations onto the HAT domain structure also highlights the key role of HAT domain integrity and cofactor binding in particular in maintaining p300 tumor suppressor activity.

Because of the involvement of p300/CBP in a growing number of cellular processes, p300/CBP is a therapeutic drug target for the development of small molecule effectors. The term "effector" refers to any agonist, antagonist, ligand or other agent that affects the activity of p300/CBP used in the assays of the present invention. Effectors can be, but are not limited to, peptides, carbohydrates, nucleic acids, lipids, fatty acids, hormones, organic compounds, and inorganic compounds. The information obtained from the inhibitor-bound p300 complex crystal structures of the present invention reveal detailed information which is useful in the design, isolation, screening and determination of potential compounds which modulate the activity of p300 proteins. Compounds that bind the L1 loop, electronegative pocket, or electronegative groove, and either sterically block substrate binding, lysine-CoA inhibitor binding, or the acetylation reaction may act as effective p300/CBP-specific inhibitors. Accordingly, the present invention provides methods for identifying a compound which modulates the activity of p300/CBP. Broadly, the methods involve designing or screening for a compound which binds to at least one amino acid residue of the L1 loop, electronegative pocket, or electronegative groove of the HAT domain of p300; and testing the compound designed or screened for its ability to modulate the activity of p300/CBP. In certain embodiments, the method of the present invention is carried

out using various *in silico*, *in vitro* and/or *in vivo* assays based on detecting interactions between the HAT domain of p300/CBP and a test compound.

In the context of the present invention, p300/CBP refers to a family member of the p300/CBP family of co-activators which have histone acetyltransferase activity. p300 is described, *e.g.*, by Eckner, et al. ((1994) *Genes Dev.* 8:869-884 and is provided in GENBANK Accession Nos. NP_001420 (human) and NP_808489 (mouse). The amino acid sequence of human p300 is set forth herein as SEQ ID NO:1. p300 is related by sequence to CBP (CREB-binding protein [CREB, cyclic-AMP responsive element binding protein]), and like CBP can stimulate transcription through activation of CREB. p300 has also been identified as a co-activator of HIF1A (hypoxia-inducible factor 1 alpha), and thus plays a role in the stimulation of hypoxia-induced genes such as VEGF. CBP is also known in the art and described, *e.g.*, by Bannister & Kouzarides ((1996) *Nature* 384:641-643) and provided in GENBANK Accession Nos. NP_004371 (human), NP_596872 (rat), and NP_001020603 (mouse). The amino acid sequence of human CBP is set forth herein as SEQ ID NO:2. For the purposes of the present invention, reference to p300 or CBP refers to human allelic and synthetic variants of p300 or CBP, and to other mammalian variants and allelic and synthetic variants thereof, as well as fragments of said human and mammalian forms of p300 or CBP. Synthetic variants include those which have at least 80%, preferably at least 90%, homology to p300 or CBP. More preferably such variants correspond to the sequence of p300 or CBP but have one or more, *e.g.*, from 1 to 10, such as from 1 to 5, substitutions, deletions or insertions of amino acids. Fragments of p300 or CBP and variants thereof are

preferably at least 20, more preferably at least 50 and most preferably at least 200 amino acids in size.

Compounds designed or screened for in accordance with the present invention can interact with at least one of the amino acid residues of the Lys-CoA inhibitor binding site, L1 loop, electronegative pocket, electronegative groove or substrate binding site of the HAT domain of p300/CBP via various heterogeneous interactions including, but not limited to van der Waals contacts, hydrogen bonding, ionic interactions, polar contacts, or combinations thereof.

As depicted in Figure 1A, the HAT domain is composed of amino acid residues 1195-1673 of p300 (SEQ ID NO:1), which correspond to amino acid residues 1231-1710 of CBP (SEQ ID NO:2). As identified herein, the L1 loop of the HAT domain, flanked by the β5-strand and α4-helix, is involved in the binding of both the acetyl-CoA and lysine moieties of the Lys-CoA inhibitor. Accordingly, in one embodiment of the present invention, a compound of the invention binds to or interacts with at least one amino acid residue of the L1 loop. In the context of the present invention, the L1 loop is composed of amino acid residues 1436-1459 of p300 (SEQ ID NO:1) or the corresponding residues of CBP, *i.e.*, amino acid residues 1472-1495. See Figure 8.

Structure analyses disclosed herein further indicate that the edges of the α3-helix/β4-strand and α4-helix/β5-strand flank the other sides of the Lys-CoA inhibitor to form the Lys-CoA inhibitor binding site. In particular, Figure 3 depicts amino acid residues of the p300 HAT domain which interact with the Lys-CoA inhibitor. As depicted, the CoA moiety of the Lys-CoA inhibitor interacts with at least Arg1410, Thr1411, Trp1466, Arg1462 and Ile1457 of p300, whereas the lysine moiety of the Lys-CoA inhibitor interacts with at least Trp1436, Tyr1397, Tyr1446, and

Cys1438 of p300. Accordingly, particular embodiments of the present invention embrace a compound which binds to or interacts with at least one amino acid residue of Lys-CoA inhibitor binding site. In the context of the present invention, the Lys-CoA inhibitor binding site is composed of amino acid residues 1395-1467 of p300 (SEQ ID NO:1) or amino acid residues 1431-1503 of CBP (SEQ ID NO:2). In particular embodiments, the Lys-CoA inhibitor binding site includes one or more of amino acid residue 1395, 1397, 1398, 1399, 1400, 1410, 1411, 1414, 1435, 1436, 1437, 1438, 1439, 1440, 1446, 1456, 1457, 1458, 1462, 1463, 1466 and 1467 of p300 (SEQ ID NO:1), or one or more of amino acid residue 1431, 1433, 1434, 1435, 1436, 1446, 1447, 1450, 1471, 1472, 1473, 1474, 1475, 1476, 1482, 1492, 1493, 1494, 1498, 1499, 1502 and 1503 of CBP (SEQ ID NO:2).

In addition to the pocket that accommodates the lysine moiety of Lys-CoA, a second pronounced and highly electronegative pocket was identified. This second pocket, referred to herein as the "electronegative pocket", is composed of at least amino acid residues Thr1357, Glu1505, Asp1625, and Asp1628 of p300 (SEQ ID NO:1), *i.e.*, amino acid residues Thr1393, Glu1541, Asp1662, and Asp1665 of CBP (SEQ ID NO:2). In addition, a narrow, shallow and electronegative groove connecting the two above-referenced pockets was identified. This groove, referred to herein as the "electronegative groove," is composed of at least amino acid residues Ser1396 and Tyr1397 of p300 (SEQ ID NO:1), or amino acid residues Ser1432 and Tyr1433 of CBP (SEQ ID NO:2). Based upon the structural and mutational analysis disclosed herein, the electronegative pocket and electronegative groove in conjunction with the pocket that accommodates the lysine moiety of Lys-CoA form the substrate binding site. Accordingly, in some embodiments,

the present invention embraces a compound which binds to or interacts with at least one amino acid residue of the electronegative pocket or electronegative groove. In other embodiments, the present invention embraces a compound which binds to or interacts with at least one amino acid residue of the substrate binding site.

In general, it is desirable that a compound of the invention interacts with 2, 3, 4, 5, 6 or up to 25 amino acid residues of the L1 loop, electronegative pocket, electronegative groove, Lys-CoA inhibitor binding site or substrate binding site of the HAT domain of p300/CBP to enhance the specificity of the compound for p300/CBP.

In accordance with the present invention, molecular design techniques or *in silico* techniques can be employed to design, identify and synthesize chemical entities and compounds, including inhibitory and stimulatory compounds, capable of binding to the HAT domain. In accordance with designing compounds which modulate the activity of the HAT domain, any suitable method for determining the crystal structure of the HAT domain can be employed. However, because the production of recombinant p300/CBP HAT domain protein in quantities necessary for crystallization is difficult using conventional methods, particular embodiments of the present invention embrace a method for producing an heterodimeric HAT complex suitable for crystallization. As exemplified herein, a heterodimeric HAT complex can be produced by expressed protein ligation of the HAT domain with the N-Cys peptide of p300/CBP, wherein limited proteolysis in the presence of an inhibitor yields an active and minimally acetylated semi-synthetic HAT domain useful for subsequent crystallization. Expressed protein ligation is well-known in the art (see, *e.g.*, Thompson, et al. (2004) *supra*) and depicted in Figure 1B.

In general, expressed protein ligation involves fusing the HAT domain (*e.g.*, amino acid residues 1287-1652 of p300 or residues 1323-1689 of CBP which lack the N-Cys peptide) to a VMA intein-chitin binding domain, purifying the fusion protein with chitin resin, and converting the fusion protein to a C-terminal thioester, *e.g.*, by treatment with MESNA. The purified fusion protein is then chemically ligated to the N-Cys peptide of the HAT domain (residues 1653-1666 of p300 or 1690-1703 of CBP) to produce an active and minimally acetylated semi-synthetic HAT domain. In particular embodiments, amino acid residues 1523-1554 of the p300 HAT domain or residues 1559-1590 of the CBP HAT domain are deleted and replaced with a potent lysine autoacetylation site as described herein to generate a loop-deleted semi-synthetic p300 HAT. Proteolysis (*e.g.*, sequential lysis with trypsin and carboxypeptidase A and B) of the resulting semi-synthetic HAT domain in the presence of an inhibitor, *e.g.*, Lys-CoA or other inhibitor (*e.g.*, identified in a screening assay) then provides a heterodimeric HAT complex suitable for crystallization in accordance with conventional techniques.

The structure of the HAT domain can be used in conjunction with computer modeling using a docking program such as GRAM, DOCK, HOOK or AUTODOCK (Dunbrack, et al. (1997) *Folding& Design* 2:27-42) to identify potential modulators of p300/CBP. This procedure can include computer fitting of compounds to the L1 loop, electronegative pocket, electronegative groove, Lys-CoA inhibitor binding site or substrate binding site of the HAT domain to ascertain how well the shape and the chemical structure of the compound will complement these sites or to compare the compound with the binding of Lys-CoA. Computer programs can also be-employed to estimate the attraction, repulsion and

stearic hindrance of the HAT domain of p300/CBP and effector compound. Generally, the tighter the fit, the lower the stearic hindrances, the greater the attractive forces, and the greater the specificity which are important features for a specific effector compound which is more likely to interact with p300/CBP rather than other classes of proteins.

Alternatively, a chemical-probe approach can be employed in the design of p300/CBP modulators or effectors. For example, Goodford ((1985) *J. Med. Chem.* 28:849) describes several commercial software packages, such as GRID (Molecular Discovery Ltd., Oxford, UK), which probe the L1 loop, electronegative pocket, electronegative groove, Lys-CoA inhibitor binding site or substrate binding site of the HAT domain with different chemical probes, *e.g.*, water, a methyl group, an amine nitrogen, a carboxyl oxygen, and a hydroxyl. Favored sites for interaction between these regions or sites of the HAT domain and each probe are thus determined, and from the resulting three-dimensional pattern of such regions or sites a putative complementary molecule can be generated.

The compounds of the present invention can also be designed by visually inspecting the three-dimensional structure of the HAT domain of p300 to determine more effective inhibitors or activators. This type of modeling is generally referred to as "manual" drug design. Manual drug design can employ visual inspection and analysis using a graphics visualization program such as "O" (Jones, et al. (1991) *Acta Crystallographica Section A* A47:110-119).

Initially effector compounds can be selected for their structural similarity to the X, Y and Z constituents of, *e.g.*, Lys-CoA by manual drug design. The structural analog thus designed can then be modified by computer modeling

programs to better define the most likely effective candidates. Reduction of the number of potential candidates is useful as it may not be possible to synthesize and screen a countless number of compound variations that may have some similarity to known inhibitory molecules. Such analysis has been shown effective in the development of HIV protease inhibitors (Lam, et al. (1994) *Science* 263:380-384; Wlodawer, et al. (1993) *Ann. Rev. Biochem.* 62:543-585; Appelt (1993) *Perspectives in Drug Discovery and Design* 1:23-48; Erickson (1993) *Perspectives in Drug Discovery and Design* 1:109-128). Alternatively, random screening of a small molecule library could lead to modulators whose activity may then be analyzed by computer modeling as described above to better determine their effectiveness as inhibitors or activators.

Programs suitable for searching three-dimensional databases include MACCS-3D and ISIS/3D (Molecular Design Ltd, San Leandro, CA), ChemDBS-3D (Chemical Design Ltd., Oxford, UK), and Sybyl/3 DB Unity (Tripos Associates, St Louis, MO). Programs suitable for compound selection and design include, *e.g.*, DISCO (Abbott Laboratories, Abbott Park, IL), Catalyst (Bio-CAD Corp., Mountain View, CA), and ChemDBS-3D (Chemical Design Ltd., Oxford, UK).

The compounds designed using the information of the present invention can bind to all or a portion of the HAT domain of p300/CBP and may be more potent, more specific, less toxic and more effective than known inhibitors of p300/CBP. The designed compounds can also be less potent but have a longer half-life *in vivo* and/or *in vitro* and therefore be more effective at modulating p300/CBP activity *in vivo* and/or *in vitro* for prolonged periods of time. Such designed modulators are useful to inhibit or activate p300/CBP activity to, *e.g.*, alter cyclic AMP-related gene

activation; histone acetyltransferase activity; or co-activation of p53, NFκB, STAT3, GATA-1, MyoD, TCF, androgen receptor, and HIV Tat.

The present invention also provides the use of molecular design techniques to computationally screen small molecule databases for chemical entities or compounds that can bind to p300/CBP in a manner analogous to the Lys-CoA inhibitor as defined by the structure of the present invention. Such computational screening can identify various groups which interact with one or more amino acid residues of the Lys-CoA inhibitor binding site of the HAT domain of p300 and can be employed to synthesize modulators of the present invention.

In vitro (*i.e.*, in solution) screening assays are also embraced by the present invention. Such assays include combining p300/CBP, the p300/CBP HAT domain (*e.g.*, as disclosed herein), or portions of the p300/CBP HAT domain (*e.g.*, sites, or fragments disclosed herein) with acetyl-CoA and a substrate (*e.g.*, H4-15 peptide) in solution and determining whether a test compound can sterically block the subsequent acetylation reaction.

Compounds which can be screened in accordance with the method of the present invention are generally derived from libraries of agents or compounds. Such libraries can contain either collections of pure agents or collections of agent mixtures. Examples of pure agents include, but are not limited to, proteins, polypeptides, peptides, nucleic acids, oligonucleotides, carbohydrates, lipids, synthetic or semi-synthetic chemicals, and purified natural products. Examples of agent mixtures include, but are not limited to, extracts of prokaryotic or eukaryotic cells and tissues, as well as fermentation broths and cell or tissue culture supernates. Databases of chemical structures are also

available from a number of sources including Cambridge Crystallographic Data Centre (Cambridge, UK) and Chemical Abstracts Service (Columbus, OH). *De novo* design programs include Ludi (Biosym Technologies Inc., San Diego, CA), Sybyl (Tripos Associates) and Aladdin (Daylight Chemical Information Systems, Irvine, CA).

Library screening can be performed using any conventional method and can be performed in any format that allows rapid preparation and processing of multiple reactions. For *in vitro* screening assays, stock solutions of the test compounds as well as assay components can be prepared manually and all subsequent pipeting, diluting, mixing, washing, incubating, sample readout and data collecting carried out using commercially available robotic pipeting equipment, automated work stations, and analytical instruments for detecting the signal generated by the assay. Examples of such detectors include, but are not limited to, luminometers, spectrophotometers, and fluorimeters, and devices that measure the decay of radioisotopes.

After designing or screening for a compound which binds to at least one amino acid residue of the L1 loop, electronegative pocket, electronegative groove, Lys-CoA inhibitor binding site or substrate binding site of the HAT domain or p300/CBP, the compound is subsequently tested for its ability to modulate the activity of p300/CBP. Such testing can be based upon whether the compound modulates the HAT activity of p300/CPB (*e.g.*, in a HAT assay), co-activation activity, or based on binding activity. To measure binding constants (*e.g.*, K_d), any suitable method known to those in the art can be employed including, *e.g.*, BIACORE analysis, isothermal titration calorimetry, ELISA with a known drug on the plate to show competitive binding,

or by a HAT activity assay. Alternatively, the compound can be co-crystallized with p300/CBP to determine the binding characteristics through X-ray crystallography techniques. See, for example, U.S. Patent No. 7,149,280 which discloses a method for identifying a ligand of a target macromolecule by obtaining an X-ray crystal diffraction pattern of a compound bound to the macromolecule crystal.

In accordance with the methods of the present invention, compounds were screened to identify modulators of p300/CBP HAT activity. Virtual library screening identified compound **7** as a potent inhibitor of p300/CBP HAT. Based upon the structure of compound **7**, several other known compounds with benzoate moieties linked to aryl groups were analyzed for inhibitory activity. These compounds and their percent inhibition of p300/CBP activity in a coupled spectrophotometric assay as well as a direct radioactive assay are listed in Table 1.

TABLE 1

Compound	Structure	% Inhibition	
		Coupled	Direct
7	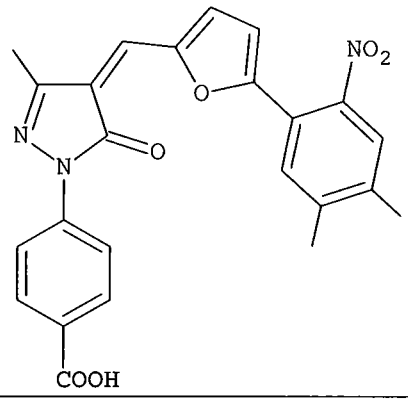	85.9%	

17.2	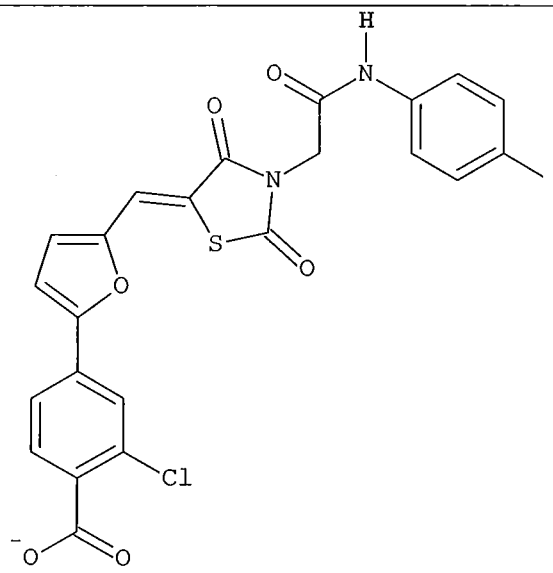		
17.3	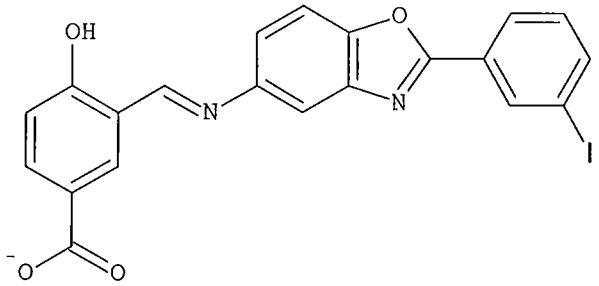		
6328730	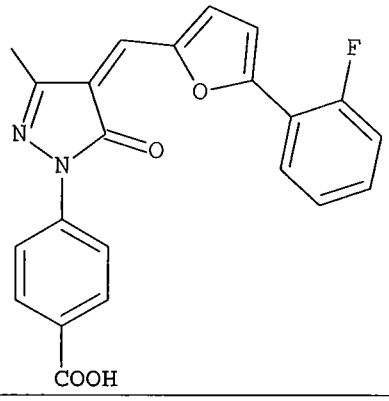	90.5%	67.9%
40174	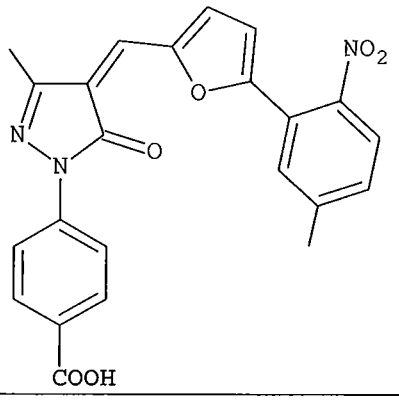	ND	79.5%

6c	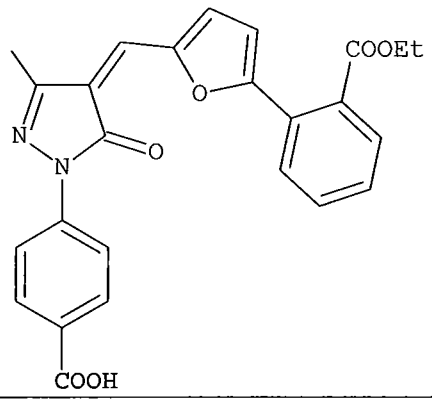	38.1%	8.3%

Pyrazolones **7**, 6328730 and 40174 were obtained commercially from Chembridge, and Interbioscreen, respectively.

Novel analogs of compound **7** were also designed, synthesized, and screened for p300/CBP inhibitory activity. These compounds and their percent inhibition of p300/CBP activity in a coupled spectrophotometric assay as well as a direct radioactive assay are listed in Table 2.

TABLE 2

Compound	Structure	% Inhibition	
		Coupled	Direct
6a	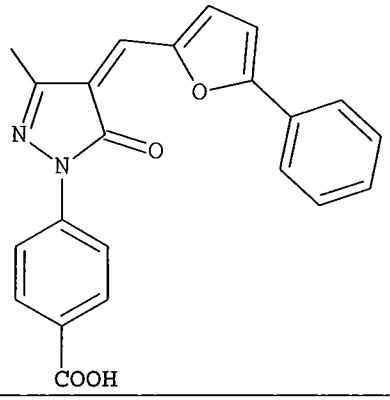	33.7%	71.5%
6b	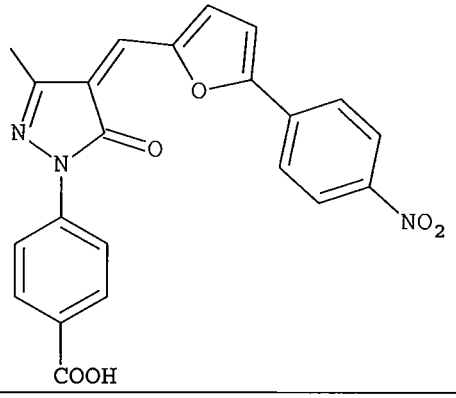	35.6%	33.8%

6d	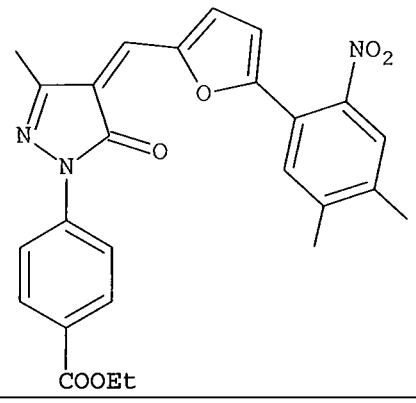	0%	ND
6e	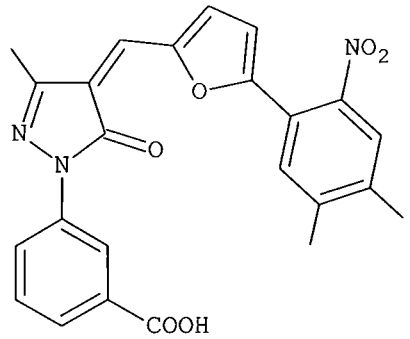	63.4%	96.4%
6f	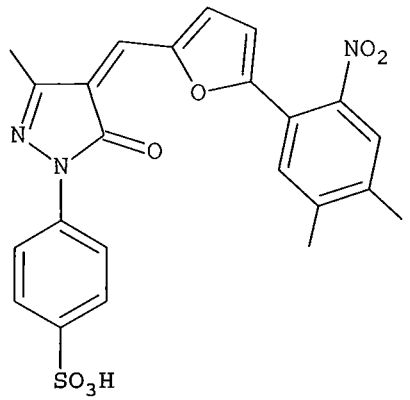	57.4%	97.2%
6g	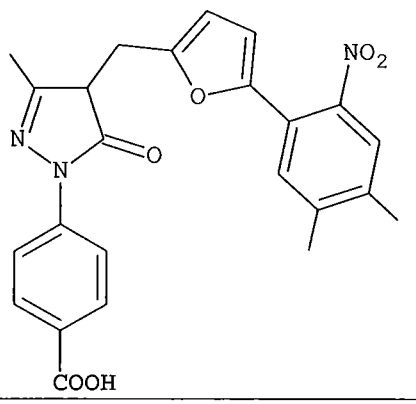	4.5%	ND

6h	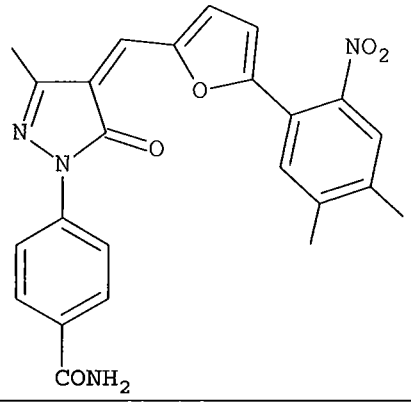	40.6%	94.7%
6i	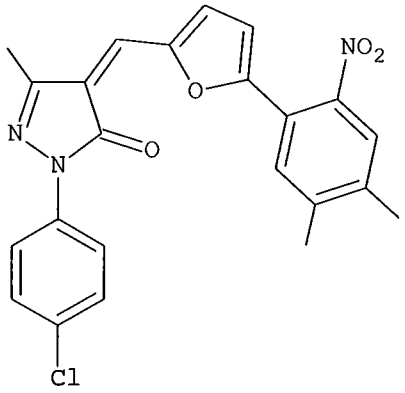	13.9%	ND
CM-26	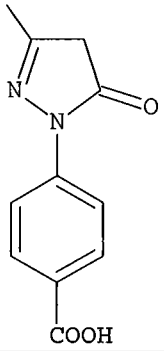	16.3%	ND
9	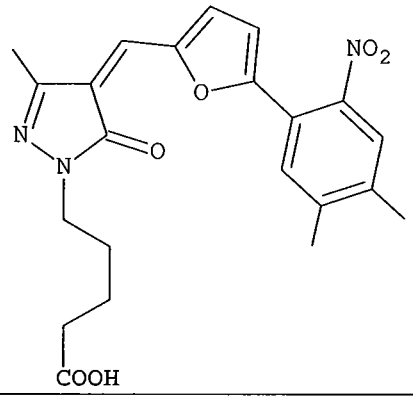	92.6%	55.8%

In accordance with particular embodiments of this invention, the compounds set forth in Table 1 and/or Table 2 are employed as inhibitors of p300/CBP activity.

Moreover, analogs, derivatives and salts of the compounds set forth in Tables 1 and 2 are also embraced by this invention. In this regard, the present invention further provides a method for making an inhibitor of p300/CBP. This method involves screening for a compound which interacts with amino acid residues Arg1410, Thr1411, Trp1466, and Tyr1467 of SEQ ID NO:1 or amino acid residues Arg1446, Thr1447, Trp1502 and Tyr1503 of SEQ ID NO:2. As depicted in Figure 11, the compounds listed in Tables 1 and 2 appear to overlap with acetyl-CoA binding and can thus be used as competitive inhibitors of acetyl-CoA binding. Accordingly, some embodiments embrace compounds of Formula I

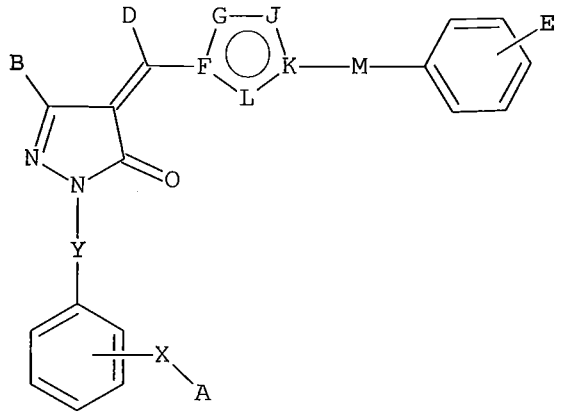

Formula I

wherein

A is COOH, $CONH_2$, SO_3H, $COCH_2NH_2$, COOR, wherein R is CH_3, C_2H_5 or alkyl;

B is CH_3, CF_3, or halogen;

D is H or CH_3;

E is any functional group or halogen;

F, G, J, K, L and M are independently any combination of C, O, S, or N;

X is $(CH_2)_n$, wherein n = 0 to 6 and said chain can contain heteroatoms (*e.g.*, O, S, or N), or X is CH_2-CH=CH-

$(CH_2)_m$, wherein m is 0 to 2 and the double bond is *cis* or *trans*; and

Y is C=O or $(CH_2)_q$ wherein q = 1 to 3.

In certain embodiments of the present invention, an inhibitor of p300/CBP is set forth in Formula II

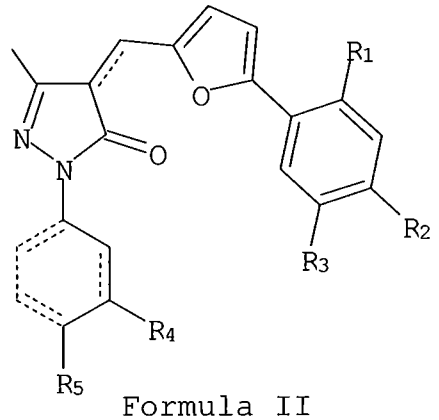

Formula II

wherein the dotted lines represent optional bonds,

R_1 is H, NO_2, or substituted or unsubstituted C_{1-4} alkyl;

R_2 and R_3 are independently H, CH_3, or NO_2;

R_4 and R_5 are independently H, CH_3, NO_2, SO_3H, halogen or substituted or unsubstituted C_{1-4} alkyl;

with the provisio that Formula I does not include a compound wherein R_1 is NO_2, R_2 and R_3 are CH_3, R_4 is H, and R_5 COOH; a compound wherein R_1 is NO_2, R_2 is H, R_3 are CH_3, R_4 is H, and R_5 COOH; or a compound wherein R_1 is COOEt, R_2 and R_3 are H, R_4 is H, and R_5 COOH.

As used herein, alkyl groups may be straight or branched chain groups of desirably 1 to 4 carbon atoms. Methyl, ethyl, and propyl including isopropyl are particular suitable alkyl groups in the compounds of the present invention. The alkyl groups of the compounds of the present invention can be substituted by one or more different groups including H, OH, CH_3, halogen, and amino groups. The number of substitutions on the alkyl group is

restricted only by the number of substitutable positions and by steric constraints.

Halogen atoms in the compounds of the present invention are desirably fluorine, chlorine, bromine or iodine.

To further evaluate the efficacy of a compound identified using the method of the invention, one of skill will appreciate that a model system of any particular disease or disorder involving p300/CBP can be utilized to evaluate the adsorption, distribution, metabolism and excretion of a compound as well as its potential toxicity in acute, sub-chronic and chronic studies.

By way of illustration, Example 12 describes a cell-based assay and animal model systems which can be used to assess the inhibition of tumor cell growth by one or more compounds of the invention. Another useful method for assessing anticancer activities of compounds of the invention involves the multiple-human cancer cell line screening assays run by the National Cancer Institute (see, *e.g.*, Boyd (1989) in *Cancer: Principles and Practice of Oncology Updates*, DeVita et al., eds, pp. 1-12). This screening panel, which involves approximately 60 different human cancer cell lines, is a useful indicator of *in vivo* antitumor activity for a broad variety of tumor types (Grever, et al. (1992) *Seminars Oncol.* 19:622; Monks, et al. (1991) *Natl. Cancer Inst.* 83:757-766), such as leukemia, non-small cell lung, colon, melanoma, ovarian, renal, prostate, and breast cancers. Antitumor activities can be expressed in terms of ED_{50} (or GI_{50}), where ED_{50} is the molar concentration of compound effective to reduce cell growth by 50%. Compounds with lower ED_{50} values tend to have greater anticancer activities than compounds with higher ED_{50} values.

Upon the confirmation of a compound's potential activity in one or more *in vitro* assays, further evaluation is typically conducted *in vivo* in laboratory animals, for example, measuring reduction of lung nodule metastases in mice with B16 melanoma (*e.g.*, Schuchter, et al. (1991) *Cancer Res.* 51:682-687). The efficacy of a compound of the invention either alone or as a drug combination chemotherapy can also be evaluated, for example, using the human B-CLL xenograft model in mice (*e.g.*, Mohammad, et al. (1996) *Leukemia* 10:130-137). Such assays typically involve injecting primary tumor cells or a tumor cell line into immune compromised mice (*e.g.*, a SCID mouse or other suitable animal) and allowing the tumor to grow. Mice carrying the tumors are then treated with a compound of the invention and tumor size is measured to follow the effect of the treatment. Alternatively, a compound of the invention is administered prior to injection of tumor cells to evaluate tumor prevention. Ultimately, the safety and efficacy of compounds of the invention are evaluated in human clinical trials.

Compounds which bind to at least one amino acid residue of the L1 loop, electronegative pocket, electronegative groove, Lys-CoA inhibitor binding site or substrate binding site of the HAT domain or p300/CBP can be used in a method for modulating (*i.e.*, blocking or inhibiting, or enhancing or activating) a p300/CBP. Such a method involves contacting a p300/CBP either *in vitro* or *in vivo* with an effective amount of a compound that interacts with at least one amino acid residue of the L1 loop, electronegative pocket, electronegative groove, Lys-CoA inhibitor binding site or substrate binding site of the HAT domain or p300/CBP so that the activity of p300/CBP is modulated. An effective amount of an effector or modulatory

compound is an amount which reduces or increases the activity of the p300/CBP by 10%, 20%, 30%, 40%, 50%, 60%, 70%, 80%, 90% or 100%. Such activity can be monitored using the methods disclosed herein, by enzymatic assays detecting activity of the p300/CBP, or by monitoring the expression or activity of proteins which are known to be regulated by p300/CBP protein (*e.g.*, p53, NFκB, STAT3, GATA-1, MyoD, TCF, androgen receptor, and HIV Tat).

Given the therapeutic potential of p300/CBP inhibitors in cancer (Iyer, et al. (2004) *Proc. Natl. Acad. Sci. USA* 101:7386-7391; Stimson, et al. (2005) *Mol. Cancer Ther.* 4:1521-1532; Zheng, et al. (2004) *Methods Enzymol.* 376:188-199), cardiac disease (Davidson, et al. (2005) *Chembiochem.* 6:162-170), diabetes mellitus (Zhou, et al. (2004) *Nat. Med.* 10:633-637), and HIV (Varier & Kundu (2006) *Curr. Pharm. Des.* 12:1975-1993), the structure disclosed herein is useful for designing and screening for more specific compounds based on, *e.g.*, the Lys-CoA scaffold. Of equal importance would be compounds that complement disease-associated mutants (Iyer, et al. (2004) *supra*) that are associated with p300/CBP HAT inactivation (Qiao, et al. (2006) *Science* 311:1293-1297).

In this regard, one of skill in the art can appreciate that modulating the activity of p300/CBP can be useful in selectively analyzing p300/CBP signaling events in model systems as well as in preventing or treating diseases and disorders involving p300/CBP. The selection of the compound for use in preventing or treating a particular disease or disorder will be dependent upon the particular disease or disorder. For example, a compound which inhibits the activity of p300/CBP will be useful in the prevention or treatment of cancer, cardiac disease, diabetes mellitus, obesity and HIV.

Prevention or treatment typically involves administering to a subject in need of treatment a pharmaceutical composition containing an effective dose of a compound identified in the screening method of the invention. In most cases this will be a human being, but treatment of agricultural animals, *e.g.*, livestock and poultry, and companion animals, *e.g.*, dogs, cats and horses, is expressly covered herein. The selection of the dosage or effective amount of a compound is that which has the desired outcome of preventing, reducing or reversing at least one sign or symptom of the disease or disorder being treated. For example, a subject with cancer (including, *e.g.*, carcinomas, melanomas, sarcomas, lymphomas and leukaemias) can experience unexplained weight loss, fatigue, fever, pain, skin changes, sores that do not heal, thickening or lump in breast or other parts of the body, or a nagging cough or hoarseness, wherein treatment with a compound of the invention can prevent, reduce, or reverse one or more of these symptoms.

Pharmaceutical compositions can be in the form of pharmaceutically acceptable salts and complexes and can be provided in a pharmaceutically acceptable carrier and at an appropriate dose. Such pharmaceutical compositions can be prepared by methods and contain carriers which are well-known in the art. A generally recognized compendium of such methods and ingredients is Remington: The Science and Practice of Pharmacy, Alfonso R. Gennaro, editor, 20th ed. Lippincott Williams & Wilkins: Philadelphia, PA, 2000. A pharmaceutically-acceptable carrier, composition or vehicle, such as a liquid or solid filler, diluent, excipient, or solvent encapsulating material, is involved in carrying or transporting the subject compound from one organ, or portion of the body, to another organ, or portion

of the body. Each carrier must be acceptable in the sense of being compatible with the other ingredients of the formulation and not injurious to the subject being treated.

Examples of materials which can serve as pharmaceutically acceptable carriers include sugars, such as lactose, glucose and sucrose; starches, such as corn starch and potato starch; cellulose, and its derivatives, such as sodium carboxymethyl cellulose, ethyl cellulose and cellulose acetate; powdered tragacanth; malt; gelatin; talc; excipients, such as cocoa butter and suppository waxes; oils, such as peanut oil, cottonseed oil, safflower oil, sesame oil, olive oil, corn oil and soybean oil; glycols, such as propylene glycol; polyols, such as glycerin, sorbitol, mannitol and polyethylene glycol; esters, such as ethyl oleate and ethyl laurate; agar; buffering agents, such as magnesium hydroxide and aluminum hydroxide; alginic acid; pyrogen-free water; isotonic saline; Ringer's solution; ethyl alcohol; pH buffered solutions; polyesters, polycarbonates and/or polyanhydrides; and other non-toxic compatible substances employed in pharmaceutical formulations. Wetting agents, emulsifiers and lubricants, such as sodium lauryl sulfate and magnesium stearate, as well as coloring agents, release agents, coating agents, sweetening, flavoring and perfuming agents, preservatives and antioxidants can also be present in the compositions.

The compositions of the present invention can be administered parenterally (for example, by intravenous, intraperitoneal, subcutaneous or intramuscular injection), topically (including buccal and sublingual), orally, intranasally, intravaginally, or rectally according to standard medical practices.

The selected dosage level will depend upon a variety of factors including the activity of the particular compound of the present invention employed, the route of administration, the time of administration, the rate of excretion or metabolism of the particular compound being employed, the duration of the treatment, other drugs, compounds and/or materials used in combination with the particular compound employed, the age, sex, weight, condition, general health and prior medical history of the patient being treated, and like factors well known in the medical arts.

A physician or veterinarian having ordinary skill in the art can readily determine and prescribe the effective amount of the pharmaceutical composition required. For example, the physician or veterinarian could start doses of a compound at levels lower than that required in order to achieve the desired therapeutic effect and gradually increase the dosage until the desired effect is achieved. This is considered to be within the skill of the artisan and one can review the existing literature on a specific compound or similar compounds to determine optimal dosing.

The invention is described in greater detail by the following non-limiting examples.

Example 1: Materials and Methods

Peptide Synthesis. Peptides CMLVELHTQSQDRF (SEQ ID NO:24) for expressed protein ligation and H4-15 (GRGKGGKGLGKGGAK; SEQ ID NO:25) for acetyltransferase assays were prepared using the solid phase peptide synthesis Fmoc strategy. The N-terminal amino group was acetylated for the H4-15 substrate peptide. Peptides were purified (>95% homogeneity) by reversed phase (C-18) high performance liquid chromatography as described previously

using a gradient of water-acetontitrile (0.05% trifluoroacetic acid) (Thompson, et al. (2001) *supra*). Electrospray mass spectrometry of peptides confirmed the correct masses.

Constructs and Semisynthetic p300 HAT. Semisynthetic proteins were prepared and purified following known procedures (Thompson, et al. (2004) *supra*). Briefly, the truncated p300 HAT domain (amino acid residues 1287-1652) or (amino acid residues 1287-1652 with an internal deletion of amino acid residues 1523-1554) containing an M1652G mutation was inserted into the pTYB2 expression plasmid (New England Biolabs, Ipswich, MA). Different point mutations were introduced into the plasmid by site-directed mutagenesis. For protein preparation, the truncated p300 HAT fused to VMA intein-chitin binding domain was expressed in *E. coli* BL21(DE3)-RIL cells at 16°C for 16 hours induced by IPTG (0.5 mM). The cells were harvested and lysed by French press in intein lysis buffer (25 mM HEPES (pH 7.9), 500 mM NaCl, 10% glycerol, 1 mM $MgSO_4$, and 2 mM PMSF). After centrifugation, the supernatant was applied to a chitin column that was extensively washed to remove unbound proteins. The immobilized fusion protein was treated with 200 mM MESNA to generate the thioester and ligated to a synthetic peptide corresponding to amino acid residues 1653-1666 (CMLVELHTQSQDRF; SEQ ID NO:24) over 16 hours at room temperature. The semi-synthetic p300 HAT was then applied to a MONO-S HR5/5 cation exchange column (Amersham Biosciences) for further purification. Following concentration, 10% glycerol was added before flash freezing in liquid N_2 and samples were stored at -80°C. Semi-synthetic proteins showed the correct mass as determined by MALDI mass spectrometry.

Crystallization and Structure Determination. To facilitate protein crystallization, the purified p300 HAT was subjected to a 2-step protease treatment. Briefly, concentrated p300 HAT was diluted to 1 mg/ml in a buffer containing phosphate-buffered saline, pH 7.4 and 5 mM dithiothreitol. Fifty μM Lys-CoA was added to the diluted p300 HAT and incubated for 30 minutes. Ten μg/ml trypsin was then added to the protein inhibitor complex at room temperature for 16 hours, and followed by protease treatment with 10 μg/ml carboxypeptidase A and B for another 16 hours. Following protease treatments, two bands corresponding to two protease-resistant p300 N- and C-subdomains were observed on SDS-PAGE gel and were further purified by anion exchange and gel filtration chromatography with MONOQ and SUPERDEX 200a, respectively. The molecular weights of the N- and C-subdomains were assessed to be ~28 kDa and ~11 kDa, respectively, by MALDI-TOF and accurate N-terminal sequences of these two subdomains were obtained by Edman degradation.

The copurified N- and C-subdomains of the p300 HAT domain were concentrated to 12 mg/ml in a buffer containing 20 mM HEPES, pH 7.4, 150 mM sodium chloride and 5 mM dithiothreitol by ultrafiltration for crystallization using hanging-drop vapor-diffusion at room temperature. Initial crystals were obtained by mixing 0.7 μl protein with 0.7 μl reservoir containing 0.1 M HEPES. pH 7.5, 20% w/v polyethylene glycol 4,000 and 10% v/v 2-propanol (Hampton Research, Aliso Viejo, CA). Crystals typically appeared in two days but were not easily reproduced and did not grow large enough for diffraction studies. Streak seeding with these initial crystals was necessary to obtain crystals with typical size of 50μmx50μmx30μm. Selenium-derived protein was crystallized under the same conditions as the

native protein. Both native and selenium-derived crystals were cryo-protected by transferring them stepwise into a reservoir solution supplemented with 5%, 10% and 15% v/v glycerol respectively, with 500 mM sodium chloride also added into the final cryo-protection solution prior to flash freezing the crystals into liquid propane cooled by liquid nitrogen for data collection. To prepare bromide-derived crystals, native crystals were cryo-protected and frozen as described above, except that sodium chloride was replaced by sodium bromide in the final cryoprotection step and crystals were only soaked for 30-60 seconds prior to freezing them (Dauter, et al. (2000) *Acta Crystallogr. D Biol. Crystallogr.* 56:232-237).

Crystallographic data from both native and derivatized crystals were collected at beamline X6A at the National Synchrotron Light Source (NSLS, Brookhaven National Laboratories). Multiple-wavelength anomalous (MAD) diffraction (Hendrickson & Ogata (1997) *Methods Enzymol.* 276:494-523) datasets were collected for selenium and bromide-derived crystals and the data was processed and scaled with the HKL2000 suite of programs (Otwinowski & Minor (1997) *Methods Enzymol.* 276:307-326). Due to crystal decay of the bromide-derivatized crystals, only a dataset at the peak wavelength for bromine was useful for phase calculation in single-wavelength anomalous diffraction (SAD). Initial phases was calculated independently for Se-MAD and Br-SAD using the programs SOLVE (Terwilliger & Berendzen (1999) *Acta Crystallogr. D Biol. Crystallogr.* 55:849-861) and SHELX followed by using the AUTOBUILD function in RESOLVE (Terwilliger (2000) *Acta Crystallogr. D Biol. Crystallogr.* 56:965-972; Terwilliger (2003) *Acta Crystallogr. D Biol. Crystallogr.* 59:38-44) and ARP/wARP (Perrakis, et al. (1999) *Nat. Struct. Biol.* 6:458-463)

respectively, which resulted in nearly identical models representing 90% of the input protein sequence. A partial model refinement in CNS (Brunger, et al. (1998) *Acta Crystallogr. D Biol. Crystallogr.* 54:905-921) with simulated annealing permitted manual building with the program O (Jones, et al. (1991) *Acta Crystallogr. A* 47(Pt 2):110-119) of additional protein residues that were not present in the initial model. Inspection of Fo - Fc difference Fourier maps at this stage facilitated the unambiguous placement of the Lys-CoA inhibitor employing the HI-CUp server (Kleywegt (2007) *Acta Crystallogr. D Biol. Crystallogr.* 63:94-100). The complete model was further refined using translation, liberation and screw-rotation (TLS) and restrained refinement in REFMAC (inn, et al. (2001) *Acta Crystallogr. D Biol. Crystallogr.* 57:122-13) implemented in CCP4i to a final resolution of 1.7 Å. The final model was checked by PROCHECK (Laskowski, et al. (1993) *J. Appl. Cryst.* 26:283-291) revealing good stereochemical parameters with no residues outside of the allowed regions of the Ramachandran plot.

HAT Assays. HAT activity was determined by either a rapid and nonradioactive HAT assay that measures the production of CoASH by its facile reaction with DTNB, or by a radioactive assay (Lau, et al. (2000) *supra*; Thompson, et al. (2000) *supra*). For the DTNB assay, fixed concentrations of acetyl-CoA (2 mM) and the H4-15 peptide (400 μM) were used to measure the k_{cat} and K_m parameters for peptides and acetyl-CoA, respectively. For the radioactive assay, the concentration of [^{14}C]acetyl-CoA was fixed at 20 μM when measuring the steady-state kinetic parameters for peptide substrates.

Example 2: Preparation and Crystallization of Semi-Synthetic p300 HAT Domain

Production of recombinant p300/CBP HAT domain protein in quantities necessary for crystallization is difficult using conventional methods because of toxicity due to aberrant acetylation of host proteins as well as heterogeneous p300 HAT autoacetylation. To overcome these challenges, a semi-synthetic human p300 HAT domain was generated using expressed protein ligation (Thompson, et al. (2004) *supra*) (Figure 1B). In this procedure, p300 amino acid residues 1287-1652 were generated, fused to a VMA intein-chitin binding domain, which can be purified on chitin resin, and then converted to a C-terminal thioester by treatment with MESNA. This p300 fragment was soluble but catalytically inactive, and its activity could be recovered by native chemical ligation to N-Cys peptide (residues 1653-1666), which produces active and minimally acetylated semi-synthetic p300 HAT. To further aid in crystallization efforts, 32 residues (1523-1554) of a proteolytically sensitive region were genetically deleted and replaced with a potent lysine autoacetylation site at 1637 with an arginine residue (Thompson, et al. (2004) *supra*). Although well-behaved by gel filtration, this loop-deleted semi-synthetic p300 HAT failed to crystallize with various ligands tested.

It was contemplated that a residual internal flexible loop was inhibiting crystallization. Therefore, the semi-synthetic p300 HAT was treated with various ratios of trypsin. Two relatively well-defined p300 HAT fragments (about 28 kDa and 11 kDa) were generated when limited proteolysis was performed in the presence of Lys-CoA, whereas protease treatment gave a more complex mixture in the absence of p300 HAT inhibitor. By mass spectrometry and

N-terminal sequencing, it was shown that the 28 kDa band corresponded to an N-terminal subdomain (N-subdomain) and that the 11 kDa band corresponded to a C-terminal subdomain (C-subdomain) and that approximately 12 amino acids were removed in addition to the 32 amino acids already genetically deleted (total removal ca. amino acids 1523-1567). The heterodimeric p300 HAT complex was prepared in the presence of Lys-CoA by carrying out an additional proteolysis of the complex with carboxypeptidase A and B and using ion exchange and gel filtration chromatography, which preserved the integrity of the complex, suggesting a stable association and structure.

Purified heterodimeric semi-synthetic p300 HAT-Lys-CoA was crystallized using hanging drop vapor diffusion and streak seeding to obtain crystals of sufficient size (50μm×50μm×30μm) for X-ray data collection. Crystals of the p300 HAT-inhibitor complex formed in spacegroup $P4_3$ with one complex per asymmetric unit cell and the structure was determined by a combination of MAD and SAD using selenomethione and bromine derivatized protein (Table 3).

TABLE 3

Data set	Se-MAD			Br-SAD	Native
	Peak	Edge	Remote	Peak	
Space group		$P4_3$		$P4_3$	$P4_3$
Unit cell dimensions (Å)					
a		61.3		61.4	61.5
b		61.3		61.4	61.5
c		101.3		101.0	101.2
Wavelength (Å)	0.9786	0.9789	0.9287	0.9193	0.9253
Resolution (Å)	50-2.0	50-2.0	50-2.0	50-1.8	50-1.7
Unique reflections	25310	25331	25271	34709	41358
Completeness (%) [a]	99.9 (100.0)	99.9 (100.0)	99.9 (100.0)	100.0 (100.0)	99.9 (100.0)
Multiplicity	6.3	6.3	6.3	6.4	5.6
I/σ	18.4 (2.4)	18.8 (2.4)	21.3 (2.2)	29.2 (3.5)	33.5 (2.6)
R_{merge} (%) [b]	8.6 (71.9)	8.4 (76.8)	8.3 (81.2)	5.6 (50.9)	4.4 (65.8)

Number of sites	6	28	
FOM/CC	0.51	0.33	
Resolution range			50-1.7
R_{cryst} (%) [c]			22.1
R_{free} (%) [d]			18.2
Number of atoms			
Protein			2596
Lys-CoA			64
Water			299
Average B-factors (Å^2)			
Protein			25.3
Lys-CoA			22.5
Water			35.1
Root mean square deviations			
Bond length (Å)			0.011
Bond angle (°)			1.466

[a] Values in parentheses are from the highest resolution shell.
[b] $R_{merge} = \Sigma|I-\langle I\rangle|/\Sigma\langle I\rangle$
[c] $R_{cryst} = \Sigma||F_o|-|F_c||/\Sigma|F_o|$
[d] $R_{free} = \Sigma_T||F_o|-|F_c||/\Sigma_T|F_o|$ (where T is a test data set of 5% of the total reflections randomly chosen and set aside before refinement).

Example 3: Overall Structure of the p300 HAT-Inhibitor Complex

The overall fold of the p300 HAT domain includes a central β-sheet composed of 7 β-strands surrounded by 9 α-helices and several loops, with the last 3 α-helices and the last β-strand coming from the C-subdomain (Figure 8). The smaller C-subdomain spans the entire structure by capping opposite ends of the larger N-subdomain with secondary structural elements that are connected by a long loop (L2) that tracks along the "bottom" side of the N-subdomain. This intimate association of the N- and C-subdomains is consistent with their protease resistance and tight heteromeric association during purification and crystallization. Within the central β-sheet the β7-strand from the C-subdomain is intercalated between the β5 and β6 strands of the N-subdomain, contributing to the integral

association between the two subdomains. On the "top" surface and at one end of the β-sheet, the α2, α5 and α6 helices from the N-subdomain and the α7 helix and a loop region from the C-subdomain form a local hydrophobic core that appears to provide a structurally stable scaffold for the cleaved autoacetylation loop that connects the α6 and α7 helices of the N- and C-subdomains, respectively, of the native protein. In the presence of the Lys-CoA inhibitor, this autoacetylation loop is presumably flexible and susceptible to protease cleavage. Helices α8 and α9 from the C-subdomain also sit on the "top" of the central β-sheet and cap the other end of the β-sheet. Helices α1, α3 and α4 of the N-subdomain line the "bottom" surface of the central β-sheet and make extensive interactions with the sheet. There are two unusually long loops in the structure that are referred to herein as L1 and L2. The L2 loop from the C-subdomain connects the β7 strand and α8 helix of the C-subdomain and spans the underside of the central β-sheet while the L1 loop is intimately associated with Lys-CoA inhibitor binding. Specifically, the Lys-CoA inhibitor binds to one edge of the β-sheet with the α3 helix and β4-strand on one side and the α4 helix and β5-strand on the opposite side. The L1 loop covers what would otherwise be the solvent exposed surface of the Lys-CoA inhibitor.

As described, deletion of residues 1653-1666 leads to loss of catalytic activity. The semi-synthetic ligation junction occurs in the middle of the C-terminal α9 helix and loss of this helix would presumably have ramifications for the integrity of the overall structure. It is however, noteworthy, that circular dichroism studies suggest that the catalytically defective, C-terminally truncated p300 HAT domain does not contain a significantly perturbed HAT

domain fold (Karanam, et al. (2006) *J. Biol. Chem.* 281:40292-40301).

Example 4: Comparison of p300 with Other HATs

A comparison of the p300 HAT domain with other HAT structures (Marmorstein (2001) *J. Mol. Biol.* 311:433-444) shows several differences and some similarities, despite the absence of detectable sequence conservation with other HATs. Specifically, an overlay of the p300 HAT domain with the HAT domains from yeast Gcn5, a member of the GCN5/PCAF family of HATs, and from yeast Esa1, a member of the MYST family of HATs, shows structural conservation within the central core region associated with acetyl-CoA cofactor binding. This structural homology corresponds to the A, B and D sequence motifs of the GNAT (Gcn5-related histone N-acetyltransferases) homology reported by Neuwald and Landsman (Neuwald and Landsman (1997) *supra*). Specifically, β-strands β1-β4, and α helices α3 and α4, show significant structural alignment within all three proteins, while β-strands β5 and β7 show additional structural alignment with Gcn5. In addition, like the Gcn5 and Esa1 HAT domains, p300 contains secondary structural elements that flank the central core acetyl-CoA binding region and appear to form the substrate binding cleft, as has been shown to be the case for the Gcn5 HAT, however, these regions structurally diverge among the three HAT domains.

Other aspects of the p300 HAT domain are very different from other HATs. In particular, the unusually long L1 loop that connects β5 and α4 and that appears to encapsulate the Lys-CoA inhibitor is a unique feature of the p300 HAT domain. Indeed, the L1 loop contributes about 30% of the total buried solvent accessible surface of 1225 $Å^2$ of the CoA portion of Lys-CoA. The tip of the L1 loop

also appears to be in position to influence protein substrate binding in a way that is distinct from other HATs. Indeed, the L1 loop buries 266 $Å^2$ of the lysine portion of the Lys-CoA inhibitor. In addition, comparison of the electrostatic surface potential of the substrate binding surfaces of the HAT domains of Gcn5, Esa1 and p300 shows significant divergence. While Gcn5 and Esa1 show deeper and more apolar substrate binding pockets, the p300 HAT domain reveals a shallow and highly acidic site consistent with the different substrate binding properties of p300 relative to other HATs.

Example 5: Structure-Guided Mutagenesis and Functional Characterization

The p300 HAT/Lys-CoA complex structure indicates a variety of residues that may be involved in substrate binding or catalysis. Catalytic residues include four tyrosines: Tyr1394, Tyr1397, Tyr1446, and Tyr1467 within about 3-8 Å of the Lys-CoA bridging acetyl carbonyl group. His1434, Ser1396 and Trp1436 are also proximal to the active site. Interestingly, among them, the Tyr1394 side-chain phenol makes a hydrogen bond with Asp1507, and Tyr1467 makes a hydrogen bond with the Lys-CoA sulfur atom. Residues that appear particularly critical for substrate binding include Arg1410 and Trp1466 that mediate CoA interactions in the structure. A shallow pocket proximal to the lysine moiety of the Lys-CoA inhibitor also indicates that the polar residue Thr1357 and the acidic residues Glu1505, Asp1625 and Asp1628 may play a role in binding to the basic protein substrates of p300. In addition, several cancer-associated amino-acid substitution mutants including Ser1650, Asp1399, and Arg1342 were analyzed. In general, amino acid substitutions of putative catalytic residues

involved conservative changes while other residues were substituted with alanines or charge reversal mutants. Figure 2 shows a comparison of the catalytic activity of several amino acid substitution mutants of putative catalytic and CoA-binding residues. A more comprehensive analysis of amino acid substitution mutants including those mentioned above are described in the subsequent sections.

The L1 Substrate Binding Loop and Inhibitor Recognition. The L1 loop is involved in the binding of both the acetyl-CoA and lysine moieties of the Lys-CoA inhibitor (Figure 3). This region of the p300 HAT domain is therefore also referred to herein as the L1 substrate binding loop. This substrate binding loop L1 adopts an ordered conformation without secondary structure, largely due to the presence of six prolines out of the 25 residues within this loop. While the extended regions of the L1 loop sits over the CoA portion of the Lys-CoA inhibitor, hydrophobic residues within the tip, or turn region, sit within a local hydrophobic pocket that is formed by apolar residues from both N- and C-subdomains. In particular, Ile1447 and Phe1448 from the L1 loop interact with residues from the α8, α9 and central β-sheet residues: Phe1361, Val1401, Phe1630, Phe1641 and to a lesser extent with non-polar regions of His1377, Tyr1397 and Arg1627. In addition, the side chains of Asp1445, His1451 and main chains of Ile1447, Phe1448 from the L1 loop form a specific hydrogen bonding network with the side chain of Asp1399 and the main chain of Ser1400 from β4. Together the L1 substrate binding loop is intimately associated with both the rest of the protein and the Lys-CoA inhibitor consistent with its resistance to proteolysis.

The Lys-CoA inhibitor binds against one edge of the central β-sheet and is flanked on the opposite site by the

L1 loop. The edges of the α3 helix/β4-strand and α4 helix/β5-strand flank the two other sides that together with the central β-sheet and L1 loop surround the inhibitor within a tunnel.

The CoA portion of the Lys-CoA makes extensive interactions with the p300 HAT domain (Figure 3). Specifically, the middle portion of the pantetheine arm of the Lys-CoA inhibitor is almost completely buried by predominantly van der Waals interactions with residues from the L1 loop, α4 and β4, and the pantetheine phosphate and 3′ phosphate oxygens make several direct and water-mediated hydrogen bond interactions from residues in the β4 strand and with the guanidinium side chain of Arg1410 from α3. As discussed, Lys-CoA is unusual in requiring its 3′-phosphate for high affinity interaction with p300 (Cebrat, et al. (2003) *supra*). In this regard, Arg1410 appears to make three hydrogen bonds with phosphates of the Lys-CoA molecule, with one involving a water-mediated and a direct hydrogen bond to the 3′-phosphate and the other being a direct hydrogen bond to the pantetheine phosphate. The importance of Arg1410 was examined by replacing it with Lys and Ala. As shown in Figure 2 and Table 4, R1410A leads to a 15-fold increase in the K_m of acetyl-CoA, but has essentially the same K_m for peptide substrate compared with the wild-type p300 HAT. Unexpectedly, R1410K p300 HAT behaves much more similarly to wild-type p300 HAT, providing a strong evidence for a critical electrostatic contribution of Arg1410. In addition, the pantetheine phosphate group of Lys-CoA makes hydrogen bonds with the hydroxyl group side chain of Thr1411 and the indole ring of the Trp1466 side chain of α3 and α4, respectively, and Trp1466 also contributes hydrophobic contacts to the pantetheine arm of the CoA moiety. The modest effect on

catalysis of the W1466F mutant reveals that the Trp1466-mediated hydrogen bond is unlikely to be very important for catalysis (Figure 2); however the hydrophobic effect mediated by the Trp1466 sidechain may be nicely captured by a Phe replacement. The adenosine ring of the CoA moiety is also stabilized by a noncanonical cation-π interaction with Arg1462 from α4 and by a conventional hydrogen bond with the main chain oxygen of Ile1457 from the C-terminal end of the L1 loop.

TABLE 4

Enzyme	K_m (μM) for H4-15	K_m (μM) for AcCoA	k_{cat} (s^{-1})	V/K ($M^{-1}s^{-1}$)†	Structural basis for the mutant residue
W.T.	164±10	40±6	4.1±0.1	25,000±1643	
Y1467F	520±30	17±2	0.030± 0.001	58±4	H-bond with Sulfur and may protonate AcCoA leaving group
Y1394F	136±30	47±9	0.47± 0.04	3456±830	Proton relay
W1436A	394±40	20±3	0.19± 0.01	482±60	Hydrophobic interaction for Lys-CoA
H1434A	151±10	88±4	0.59± 0.02	3910±290	Proton replay
R1410A	190±40	657±90	1.2±0.1	6263±1300	H-bond with 3′ and pantetheine phosphate
R1410K	156±40	74±6	1.4±0.1	8718±2200	
D1625R	640±70	NM‡	3.6±0.2	5668±690	Contribute to the negative surface of the peptide binding site
D1628R	>1000	NM‡	UD*	~2100**±90	
E1505R	>1000	NM‡	UD*	~2000**±40	
T1357R	294±50	NM‡	3.9±0.3	13163±2491	Located at the peptide binding site
T1357L	111±20	NM‡	2.1±0.1	18739±3550	
D1625R/D1628R	>1000	40±7	UD*	~1162**±60	Double mutant
E1625R/D1625R/ D1628R	>1000	461±40	UD*	~232**±10	Triple mutant

*UD: Undetectable. ‡NM: Not measured.
†V/K was calculated using peptide K_m.
**V/K was calculated using a linear fit.

The lysine component of the Lys-CoA inhibitor also makes extensive interactions with the p300 HAT domain. Specifically, the ε nitrogen atom makes a hydrogen bond with the main chain oxygen of Trp1436. The amine group that caps the carboxyl end of the lysine backbone, presumably mimicking the backbone position of the Lys -1 amino acid, forms a hydrogen bond with the hydroxyl group of Tyr1397. Three hydrophobic residues, Tyr1397 from β4, and Trp1436 and Tyr1446 from the L1 loop together with Cys1438 also from the L1 loop form a hydrophobic subtunnel that interacts with the aliphatic portion of the lysine side chain.

Substrate Binding. In addition to the pocket that accommodates the lysine moiety of Lys-CoA, presumably mimicking the lysine side chain from native protein substrates, a second pronounced and highly electronegative pocket is present about 10 Å away from the substrate lysine. Because p300 substrates show a strong preference for the presence of a Lys or Arg side-chain two to three residues downstream or upstream of the primary acetylation site (Thompson, et al. (2001) *supra*) (Figure 4), the possibility that this region might be important for the binding of protein substrates was considered. Consistent with this possibility is the presence of a narrow, shallow and electronegative groove connecting the two pockets. The wall of one side of the groove is composed of Ser1396 and Tyr1397. The negative potential of the second pocket is largely formed by the side chain atoms of residues Thr1357, Glu1505, Asp1625, and Asp1628. To examine if these regions are important for substrate binding, single, double, triple and quadruple amino acid mutagenesis experiments were carried out on the mentioned residues. These mutations were designed to (1) either occlude or change the charge state of the groove or the first pocket, (2) fill the cavity or reverse the negative charge of the second pocket.

For the first strategy, since it was shown that S1396A does not decrease activity (Figure 2), S1396R/Y1397R and S1396R/Y1397R double mutants of p300 HAT were generated to perturb the groove. Both mutants showed severely decreased p300 HAT activity (>50-fold), indicating the importance of the groove for peptide substrate binding (Figure 5). For the second strategy, the T1357L replacements lead to rather modest V/K effects (Table 4), indicating that the second pocket may not be deeply engaged by peptide substrate residues. For charge reversal mutagenesis analysis, the

single mutant D1625R showed an increased peptide substrate K_m and a V/K decrease of about 5-fold, while D1628R and E1505R mutant proteins displayed more pronounced effects; V/K was decreased by 12-fold and the K_m for the H4-15 peptide substrate was too high to measure (Figure 5 and Table 4). The double, triple, and quadruple mutations showed partially additive effects (Figure 5 and Table 4). The D1625R/D1628R double mutant protein showed a 20-fold drop in V/K whereas the K_m of acetyl-CoA was unchanged compared to that of wild-type p300 HAT. The E1505R/D1625R/D1628R triple mutant displayed a more dramatic V/K reduction; however, the acetyl-CoA K_m for this triple mutant was also elevated, indicating slight structural perturbation (Figure 5 and Table 4). Thus, the D1625R/D1628R p300 HAT mutant was selected for further analysis of substrate residue preferences.

To test the influence of electrostatic interactions on substrate sequence selection, the steady state kinetic parameters for several synthetic H4 tail peptide analogs was determined (listed in Table 5). In H4-15, there are two other basic residues (Lys5 and Lys12) near the target Lys8. It has previously been shown that either one of the nearby Lys (or Arg replacements) is sufficient to permit efficient acetylation by full-length p300 (Thompson, et al. (2001) *supra*). Here, the effects of replacing Lys5 and Lys12 with Ala, the neutral residue hydrogen bonding citrulline, or Asp were compared for wild-type and mutant p300 HAT as indicated in Table 5. Analysis of the single lysine substrate, analogous to the Lys-CoA component, which contains both amino and carboxyl groups derivatized as amides (Table 5), was also conducted. K_m of these substrates were generally too high to be measured (>1000 μM) under the experimental conditions, highlighting the important role of

the nearby positively charged residues for substrate interaction. As shown Table 5, the 22-fold V/K difference between wild-type p300 HAT protein and the D1625R/D1628R mutant for H4-15 substrate dropped to 6-fold when using Ac-Lys-NH2 as substrate. The smaller V/K drop in activity with Ac-Lys-NH2 substrate indicates that a key role of Asp1625 and Asp1628 is to assist in recruiting the basic residues of H4-15 by electrostatic interaction. Consistent with this idea, H4-12$^{K5A/K12A}$ or H4-12$^{K5Cit/K12A}$ which lack proximal basic residues but contain neutral hydrogen bonding residues show kinetic behavior similar to that of Ac-Lys-NH2 (Table 5). However, with H4-15$^{K5D/K12D}$ as substrate, wild-type and D1625R/D1628R p300 HAT displayed almost equal (within 2-fold) acetyltransferase activity. Taken together, these data indicate that the second highly electronegative pocket binds to the proximal basic residue (Lys or Arg) and facilitates the acetyltransferase reaction. However, the loss of 6-fold in V/K for neutral H4 substrates H4-12$^{K5A/K12A}$ or H4-12$^{K5Cit/K12A}$ or Ac-Lys-NH2 indicates that the double mutant may also interfere with the overall surface charge of the nearby first pocket as well.

TABLE 5

Peptide	Peptide Sequence	SEQ ID NO:	V/K($M^{-1}s^{-1}$) for W.T.	V/K($M^{-1}s^{-1}$) for D1625R/D1628R
H4-15	GRG**K**GG**K**GLG**K**GGAK	25	25000±1643	1162±60
H4-15(K5D/K12D)	GRG**D**GG**K**GLG**D**GGAK	26	636±40	422±20
H4-12(K5A/K12A)	RG**A**GG**K**GLG**A**GA	27	3824±180	515±15
H4-12(K5X/K12A)	RG**X**GG**K**GLG**A**GA*	28	5247±260	738±20
Ac-Lys-NH_2	CH_3CO-NH-Lys-$CONH_2$	-	1843±50	326±10

*X=citrulline.

Autoinhibition. Although the lysine-rich autoacetylation loop of the p300 HAT domain is not present

in the structure disclosed herein, it is contemplated that it may fold back *in cis* onto the highly electronegative surface of the p300 HAT domain that is proximal to the lysine binding site. Such a nonspecific electrostatic interaction is probably strong enough to prevent the binding of other substrates until intermolecular autoacetylation of the loop occurs. Autoacetylation of multiple sites within the loop, which is known to occur, may function to neutralize the lysine-rich loop such that protein substrates may compete with it for binding to p300. Though most of the acetylated lysine residues were genetically or proteolytically removed, there were some acetylated lysines (Lys1336, Lys1499, Lys1473, Lys1637) that remained (Thompson, et al. (2004) *supra*). These lysine residues are all located at the surface, which supports an intermolecular autoacetylation model (Karanam, et al. (2006) *supra*).

Catalytic Mechanism. As discussed, studies on the p300 histone acetyltransferase reaction show conflicting evidence regarding the potential of an acetylated covalent intermediate. The catalytic relevance of the heterodimeric structure here is indicated by the heterodimeric stability through two chromatographic separations, its similarity in CoA binding to other acetyltransferases, and by site-directed mutagenesis of key active site residues contributing to turnover. The X-ray structure shows a number of potential nucleophilic residues (Ser/His/Tyr) in proximity to the predicted position of the acetyl-CoA carbonyl carbon but mutagenesis of any of these residues fails to fully abolish catalytic activity, as would be predicted for an obligate catalytic intermediate. Moreover, it has been demonstrated with acetyl-coenzyme A affinity labeling-based reagents that these do not target any

critical residue for catalysis. Given the high affinity of the partial bisubstrate analog Lys-CoA for p300 HAT, it is contemplated that the protein conformation captured in the structure corresponds to a catalytic state indicating direct passage of the acetyl group from acetyl-CoA to the substrate lysine.

It is unclear why bisubstrate analogs with longer peptide moieties are weaker binders. For example, H4-CoA-20, a bisubstrate analog composed of 20 residues of the histone H4 tail, inhibits p300 more than 20-fold more weakly than Lys-CoA (Lau, et al. (2000) *supra*) In contrast, based on studies herein and previously (Thompson, et al. (2001) *supra*), the histone H4 tail peptide H4-20 is indeed processed at least 15-fold faster than Ac-Lys-NH2 (Table 5). If a classical ternary complex mechanism were operative, then more authentic bisubstrate analogs would be expected to bind to p300 more tightly than the primitive Lys-CoA analog, as occurs with PCAF/GCN5. It is believed that a "hit-and-run" or Theorell-Chance (T.-C.) acetyl transfer mechanism (Segel (1975) *Enzyme Kinetics*) could account for such behavior. In the T.-C. mechanism, there is no stable ternary complex as formed in standard sequential mechanisms (Figure 6A). Rather, after the acetyl-CoA binds, the peptide substrate associates weakly with the p300 surface allowing the lysyl residue to snake through the p300 tunnel and react with the acetyl carbon. It is contemplated that a conformational change is associated with acetyl transfer and that this post-reaction state is captured in the structure disclosed herein. This post-reaction conformation further weakens peptide-enzyme interactions, somewhat analogous to, but more extreme than a loop displacement model suggested for PCAF/GCN5 (Poux, et al. (2002) *supra*; Zheng, et al. (2005b) *Biochemistry* 44:10501-

10509). Thus, the "partial" bisubstrate analog Lys-CoA rather than the apparently more complete structure H4-CoA-20 is a more faithful mimic of the T.-C. reaction coordinate of p300, and the X-ray structure captures this reactive state. It is noted, however, that the parallel line pattern previously observed in a steady-state two substrate kinetic analysis of p300 (Thompson, et al. (2001) *supra*) is not inconsistent with a T.-C. mechanism since the acyl transfer from a thioester to an amine is effectively irreversible thermodynamically.

The precise role of various residues in facilitating the chemistry of acetyl transfer is indicated by mutagenesis and the observed structure. Steady-state kinetic analysis of Y1394F p300 HAT showed that the loss in acetyltransferase activity for this mutant was due to a decrease in k_{cat} with insignificant K_m effects. His1434A showed a 7-fold lower k_{cat} compared with that of wild-type p300 HAT. W1436A was 50-fold slower and Y1467F was more than 400-fold slower than wild-type p300 HAT. Most of the reduction was due to a drop in k_{cat}, indicating an important effect on the chemical step in acetyl transfer. The most critical residue is Tyr1467 (Table 4). Mutation of Tyr1467 results in a 430-fold reduction in V/K. This residue forms a direct hydrogen bond to the sulfur atom of Lys-CoA and is predicted to play a key orienting role as well as general acid function in protonating the leaving group. It is noteworthy that Y1467F showed a mildly depressed acetyl-CoA K_m relative to wild-type. This indicates that ground state hydrogen bonding energy between the Tyr phenol group and the acetyl-CoA sulfur was modest and a source of strain, characteristic of a form of enzymatic rate enhancement known as ground-state destabilization (Scheibner, et al. (2002) *J. Biol. Chem.* 277:18118-18126). A related role for

a Tyr has not been observed in other HATs but has been noted in serotonin N-acetyltransferase (Scheibner, et al. (2002) *supra*).

A second key residue is Trp1436. Mutation of Trp1436 into Ala reduced k_{cat}/K_m by 50-fold (Table 4). The Trp1436 indole side-chain appears to play a key role in guiding the Lys side chain into attacking acetyl-CoA by van der Waals contact. By contributing to the hydrophobic environment (formed by Tyr1397, Ty1446, Cys1438 and Trp1436) in the active site, it also likely helps reduce the Lys pK_a below its native level of 10. This would serve to enhance catalysis by biasing the substrate Lys to the neutral amine which is necessary for attack. Although the backbone carbonyl of Trp1436 makes an H-bond with the ε-amino hydrogen of Lys-CoA, there is no obvious catalytic base in contrast to other HATs which are believed to require acidic residues playing this role. However, as discussed with serotonin N-acetyltransferase, the spontaneous reaction between a neutral amine and thioester is predicted to be very fast once the enzyme can template their association in correct orientation (Scheibner, et al. (2002) *supra*; Zheng, et al. (2004) *Methods Enzymol.* 376:188-199). Roles for polar residues for guiding the protons out of the active site are indicated for His1434 and Tyr1394 and/or Asp1507 which contribute modestly to catalysis (Table 4). An analysis of pH-rate profiles in the wild-type reaction (Figure 6B) and selected mutants (data not shown) fails to account for the important pK_a of 8.5 which we speculate may be the substrate Lys epsilon-amine group. Based on the discussion above, a catalytic mechanism is illustrated in Figure 6A.

Disease Mutations. The structure of p300 HAT permits a more detailed understanding of the enzymologic mutations

that have been observed in a number of human disease states. There are now several reports of various point mutations in p300/CBP HAT domain being observed in human cancers and Rubinstein-Taybi syndrome but these have not been characterized with enzyme kinetic studies. Such p300/CBP mutations include R1378P in CBP (R1342P in p300) in Rubinstein-Taybi syndrome (Murata, et al. (2001) *Hum. Mol. Genet.* 10:1071-1076), D1399Y in p300 in primary colon cancer (Muraoka, et al. (1996) *supra*), S1650Y in p300 in pancreatic cancer (Gayther, et al. (2000) *supra*), and R1446C (R1410 in p300), W1472C (W1436 in p300), G1411E (G1375 in p300) in CBP in human lung cancer (Kishimoto, et al. (2005) *supra*). The importance of Arg1410 and Trp1436 has been discussed above, and it is likely that replacement of these critical residues by Cys will severely decrease p300/CBP HAT activity as was observed with Ala substitutions. Arg1342 is in the middle of the α2 helix, and replacement by Pro will interrupt the helix, and it is expected that this helical destabilization would disrupt the β1-β2 interaction of the core domain. Indeed, enzymatic analysis shows that a R1342P mutation results in at least a 50-fold reduction in acetyltransferase activity compared with wild-type p300 HAT (Figure 7). In contrast, R1342K and R1342A p300 HAT mutants both show only modest 3-4-fold rate reductions, and these Arg replacements would be less likely to disrupt helical secondary structure (Figure 7). Asp1399 is a key residue of the hydrogen bonding network between the substrate binding loop L1 and the β4 core domain where it forms a direct interaction with His1451. Mutagenesis analysis shows that the D1399Y, D1399N, and D1399A p300 HAT mutants all have very low activity (<1% wt p300 HAT activity) (Figure 7), indicating that the L1 loop interaction with the core domain requires the negatively

charged side chain of Asp1399 to form a strong hydrogen bond with His1451. Ser1650 is located at the upper middle portion of α9. It is expected that the bulkier side-chain found in S1650Y will not be accommodated by the limited space available around the tight turn region between α8 and α9, thereby interfering with the conformation of the final two α-helices, which themselves appear crucial because of their interactions with the L1 loop (the C-terminal truncated protein has very low activity probably for the same reason). As expected, S1650Y p300 HAT was greatly impaired catalytically (50-fold rate reduction), whereas the smaller replacement found in S1650A led to very similar catalytic activity compared to wild-type p300 HAT (Figure 7). Although G1375E p300 HAT was not prepared, it is clear from the structure that a Glu substitution here would disrupt the appropriate positioning of the L1 loop for substrate binding (Figure 7).

Example 6: p300 L1 Loop

The L1 loop (between β5 and α6, amino acid residues 1436-1459 SEQ ID NO:1) is a specialized feature of p300 HAT which serves as a lid for Lys-CoA. Based upon structural analysis, a related loop was identified within the yeast HAT RTT109 which is overall a rather close structural homolog of p300/CBP (despite very limited sequence homology). Based on the structure (Figure 3), the L1 loop appears to be relevant for either substrate positioning, acetyl transfer, and/or product release. Thus, in addition to Trp4136Ala and Tyr1446Phe point mutations, a series of p300 HAT point mutants within the L1 loop are prepared and the kinetics (k_{cat}, K_m measurements, viscosity effects) and binding properties using acetyltransferase assays and fluorescence binding assays with CoA analogs (CoASH,

acetonyl-CoA, Lys-CoA) are carried out. L1 residues that appear to be directly interactive with Lys-CoA (Ala1437, Cys1438, Pro1439, P1440, Lys1456, Pro1458) as well as residues that may be important for loop flexibility (Pro1439, Pro1440, Pro1458) are selected for Ala scanning (or Gly for Ala1437). To investigate regulation, it is determined how loop autoacetylation, which stimulates the wild-type enzyme, affects the kinetics of particular mutants. Outcomes of interest for these experiments would be the identification of key residues that affect the rate of acetyl transfer (k_{cat} drop or change in viscosity effect), the affinity for CoA or peptide, selective effects on Lys-CoA binding or sensitivity to autoacetylation. Pro to Ala (or Gly) mutants are expected to alter the loop flexibility and provide insights into the backbone effects of these residues on loop conformation. Complementary experiments involve obtaining X-ray structures of p300 HAT in complex with CoASH and acetonyl-CoA to determine how the L1 loop and P1 pocket are influenced by the Lys-side chain. Taken together, these studies allow a more complete understanding of the relationship between structure and mechanism of p300/CBP and how autoacetylation exerts its effect on catalysis. These experiments are also relevant in the comparative biochemistry of yeast RTT10999 and p300/CBP, which as mentioned are unique in containing the L1 loop. A practical result from these L1 mutant studies is the identification of mutants that are less potently inhibited by Lys-CoA (and other inhibitors) but still retain robust acetyltransferase activity. The application of such mutants in cellular studies in "knock-in" type experiments allows for the discrimination between the biological functions of p300 and CBP HATs by permitting selective enzyme inhibition.

Example 7: p300 HAT in Protein-Protein Interactions

The p300 HAT structure shows a negatively charged pocket (P2) near the Lys moiety of Lys-CoA and has led to the plausible notion that basic substrates interact in this pocket. It is contemplated that the b-ZIP domain of ATF2 which shows affinity for the loop-deleted or autoacetylated p300 HAT and is an *in vitro* p300 substrate may interact with the p300 P2 pocket. It has been shown that two Asp residues (Asp1625, Asp1628) may be central to the preference for basic peptide substrates based on mutagenesis studies with the Asp-Asp/Arg-Arg variant. Accordingly, related experiments can be carried out with the ATF2-b-ZIP domain to determine whether mutation of these residues affects p300 HAT binding or acetylation of this transcription factor. Pull-down experiments as well as acetyltransferase assays are carried out on the Asp-Asp/Arg-Arg p300 HAT to see if GST-ATF2-bZIP shows differential interaction with the P2 mutant, as expected. Wherein the Asp-Asp/Arg-Arg mutant does not show reduced interaction with ATF-2-b-ZIP, this indicates an alternate p300 region of interaction. In either case, co-crystallization of p300 HAT with ATF2-b-ZIP is performed to determine the high resolution structural basis of interaction.

Regarding histone peptide substrate recognition by p300, studies with bisubstrate analogs, structure, and steady-state kinetics indicate that co-crystallization with H4 peptide or an H4-CoA-20 analog are unlikely to reveal relevant interactions because they are weak ligands. To circumvent this, H4-CoA-20 variants with extended linkers between peptide and CoA (L, X, Z; see Figure 9) are employed. A compound with a longer and flexible linker

between the CoA and the H4 tail peptide is expected to place the H4 peptide moiety near the histone substrate's initial encounter surface on p300, permitting capture by X-ray crystallography. After synthesizing the compounds shown in Figure 9, their potency is evaluated as p300 HAT inhibitors. The most potent compounds could indicate that dual occupancy of the p300 HAT 'Lys-CoA tunnel' as well as the adjacent 2-Asp pocket P2 is possible. This is determined by making H4 variants that replace the basic residues Lys5 and Lys12 as well as testing the p300 Asp-Asp/Arg-Arg mutant enzyme. Crystallographic analysis with the novel H4-CoA conjugates can also be performed.

Using cell co-transfection and *in vitro* enzymatic experiments, it has been found that a transcription factor called MAML1, critical in Notch signaling can activate full-length p300 HAT and also induce its hyper-autoacetylation. Like many transcription factors, it is known that MAML1 can bind to the p300/CBP C/H3 domain. It is contemplated that engaging the C/H3 domain with MAML1 relieves an intramolecular autoinhibitory interaction between the p300 HAT domain and the C/H3 domain (Figure 1A). To demonstrate this, a *trans* interaction between p300 HAT and recombinant C/H3 domain is shown by examining the ability of the C/H3 domain to modulate p300 HAT domain activity and testing for affinity using pull-downs.

Example 8: Analysis of the p300 Autoacetylation Loop

To interrogate the regulatory autoacetylation loop in p300 HAT, a circularly permuted protein domain is employed. Such a circular permutation involves linking the natural N- and C-termini (residues 1287 and 1666) of the HAT domain and creating new termini at 1565 (N-terminus) and 1520 (C-terminus). This construct is then fused to an intein

through its new C-terminus and the thioester generated is ligated to synthetic peptides containing the key autoacetylated lysines. This approach is particular useful because of the close proximity between the natural N- and C-termini; the p300 HAT crystal structure indicates that these termini are a mere 15 Å apart. Moreover, it has been demonstrated that the unlinked N- and C-subdomains of p300 HAT form a very stable complex, which also supports the use of circular permutation. In generating this circularly permuted p300 HAT, several linker lengths (6-10 residues, Gly rich linkers) can be tested to optimize expression. Because p300 HAT activity is toxic to *E. coli*, the production of the p300 Tyr1467Phe catalytically impaired mutant can be analyzed first. While this mutant will have reduced utility in acetyltransferase studies, it can be employed to assess the influence of the ligated regulatory loop (amino acid residues 1520-1565) on protein-protein interactions in binding studies. Ligation with various mono, di, and triacetylated regulatory segment peptides can be used to explore site-specific modifications on interaction. After completion of experiments on inactive circularly permuted p300 HAT, investigations with the non-catalytically impaired HAT are carried out. To limit toxicity from host protein p300 acetylation, the catalytically active HAT is coexpressed with Sir2 deacetylase. While autoacetylation of several residues in the circularly permuted p300 HAT (outside the regulatory loop which is installed *in vitro*) is likely, as demonstrated herein, these sites are not very influential on p300 HAT activity. With the semi-synthetic circularly permuted p300 HAT proteins in hand, kinetic parameters of the various site-specifically acetylated forms are measured. These studies generate unique and important new

information on how p300/CBP is regulated. If functional effects conferred by the unilaterally attached regulatory segment are not observed, the free (C-terminal end) can be linked by native chemical ligation to the new N-terminus of the circularly permuted protein. This can be achieved by generating a C-terminal thioester synthetic segment and an N-Cys on the N-terminus using Factor Xa cleavage or by a *trans*-splicing strategy.

As an alternative approach to generating a circularly permuted protein domain, a heterodimeric p300 HAT is generated by producing separate non-attached segments, which are co-expressed in *E. coli*. The N-subdomain is fused to an intein to allow ligation to regulatory segment peptides. The heterodimers thus produced would then be used in binding and catalytic studies as described for the circularly permuted protein.

Example 9: Virtual Library Screening of p300/CBP

Regulatory molecules of p300/CBP HAT were identified by using the coordinates of the p300 HAT-Lys-CoA crystal structure and systematically docking into the active site (in the Lys-CoA binding region) the structures of ~2 million commercially available compounds (from the Chembridge library) *in silico* via ICM software algorithm. The top 200 compounds were selected, which also had favorable drug-like properties (MW<500, logP = 1-6), and screened against p300 HAT using a spectrophotometric coupled assay that measures CoASH production in real-time. After secondary and tertiary screens (including a direct, radioactive assay that measures ^{14}C-incorporation from acetyl-CoA into H4 tail peptide), three compounds (**7**, **17.2** and **17.3**) were identified, which had IC_{50}s less than 20 μM, *e.g.*, the IC_{50} of **7** was 3.09 ± 0.62 μM. Moreover, **7** was

shown to exhibit competitive inhibition against acetyl-CoA (Figure 10A) and mixed-type inhibition with H4-15 substrate (Figure 10B).

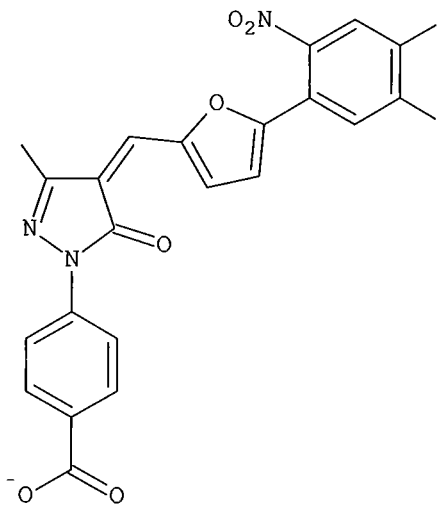

7

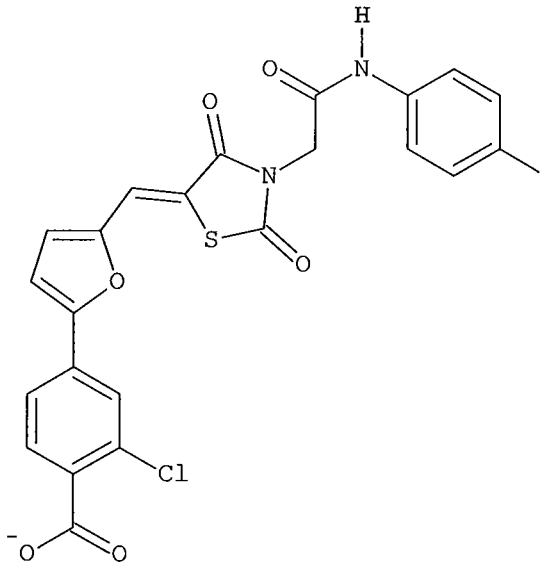

17.2

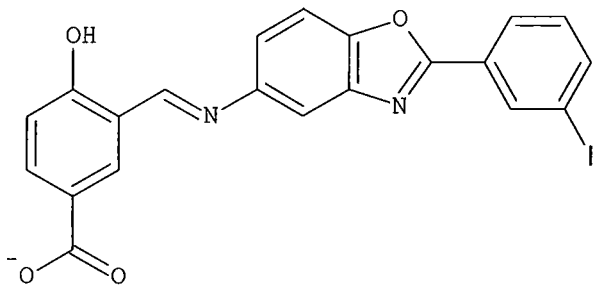

17.3

The chemical structures and purity of these three compounds were analyzed by NMR and mass spectrometry. It is noteworthy that these compounds contain a benzoate moiety linked to a series of aryl groups, which based on the computational docking (Figure 11) overlaps with CoA binding.

Example 10: Mechanistic Analysis of p300/CBP HAT Inhibitors

The three small molecule p300 HAT inhibitors (**7**, **17.2** and **17.3**) identified using virtual library screening provided new leads for further development. Based upon the

docking model of binding of compound **7** (Figure 11) and pattern of competitive inhibition of compound **7** versus acetyl-CoA (Figure 10A), it is expected that analogs of compound **7** will compete for binding with acetyl-CoA. Similarly, based upon the pattern of mixed-type inhibition of compound **7** versus peptide substrate (Figure 10B), it is expected that analogs of compound **7** exhibit non-competitive binding. Compounds that are found not to be linear competitive inhibitors vs. acetyl-CoA (studies indicate that **7** is competitive with K_i = 400 nM) are likely binding differently from the proposed docking model. From the docking model of **7** to p300 HAT (Figure 11), important hydrogen bonding roles are indicated for the side-chains of Arg1410, Thr1411, Trp1466 (all interacting with the inhibitor carboxylate) as well as the side-chain of Tyr1467 (hydrogen bonding to the nitro group). While Arg1410 and Tyr1467 are critical for CoA binding and/or catalysis, mutation of Trp1466 is well-tolerated. To explore the specificity of the small molecule HAT inhibitors, these compounds are tested against other acetyltransferases (PCAF, AANAT, RTT109, EsaI), which assists in the prioritization of candidates for pharmacologic applications.

Indeed, it was demonstrated that compound **7** was specific for p300 HAT (85.9% inhibition) compared to AANAT (4.8% inhibition) and PCAF (0% inhibition).

Example 11: Synthetic Derivation of p300/CBP HAT Inhibitors

Synthesis of congeners of **7** involved the use of Knoevenagel condensation of furanyl-aldehyde derivatives with a set of pyrazolone building blocks.

*General Procedure for Synthesis of 1-Aryl-3-Methyl-Pyrazol-5-One (**3**).* 1-Aryl-3-methyl-pyrazol-5-one **3** was

synthesized following a modified literature procedure (Scheme 1). (Kim & Lee (1991) *Bull. Korean Chem. Soc.* 12:376). A suspension of ethyl acetoacetate (2.8 mmol) and corresponding arylhydrazine (**2**, 3.3 mmol) in glacial acetic acid (30 ml) was stirred at reflux for 24 hours. The reaction mixture was concentrated and the solid precipitated out was filtered and washed with dichloromethane to remove traces of acetic acid. Yield 65-73%. **3b** was synthesized by esterification of **3a** in ethanol and purified by column chromatography using dichloromethane as eluent.

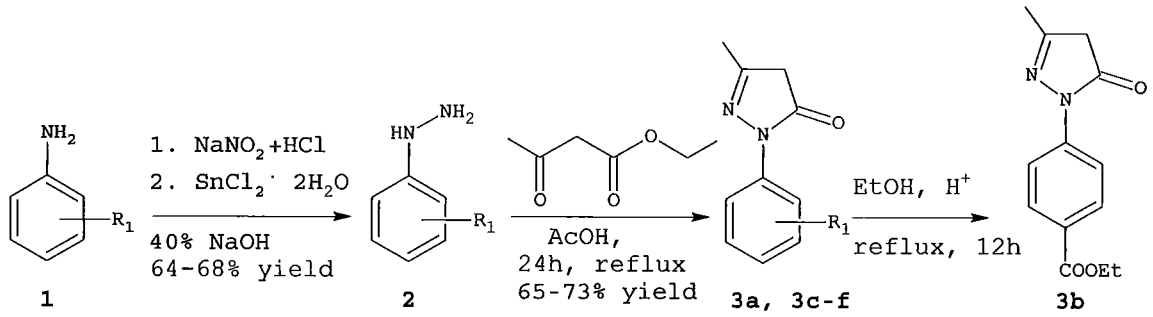

Scheme 1

wherein R_1 is 4-COOH (**3a**), 4-COOEt (**3b**), 4-$CONH_2$ (**3c**), 3-COOH (**3d**), 4-SO_3H (**3e**), 4-Cl (**3f**).

1-Bromo-4,5-dimethyl-2-nitrobenzene **4a** was synthesized in 81% yield using Sandmeyer reaction on 4,5-dimethyl-2-nitroaniline following a known procedure (Scheme 2)(Langner, et al. (2005) *Chem. Eur. J.* 11:6254). Ethyl 2-iodobenzoate **4d** was prepared from esterification of corresponding halo-acid by refluxing in ethanol for 24 h. Pure product was obtained in 85% yield by column chromatography using dichloromethane as eluent.

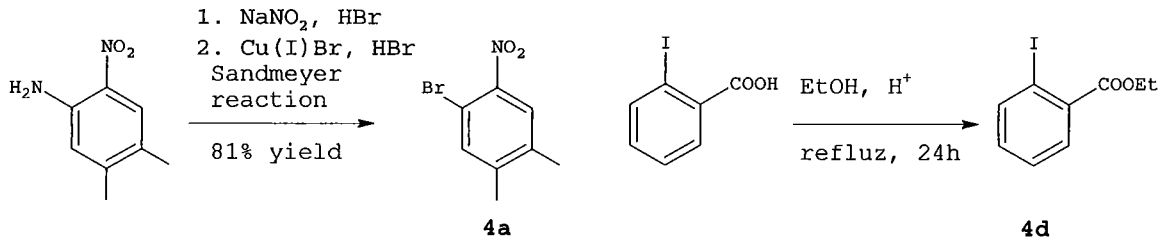

Scheme 2

*General Procedures for Synthesis of 5-Aryl-2-Furaldehydes (**5**).* 5-Aryl-2-furaldehyde **5** was synthesized from Suzuki coupling of 5-formyl-2-furanboronic acid and corresponding aryl halides **4** in 72-75% yields following a literature procedure (Scheme 3) (Hosoya, et al. (2003) *Bioorg. Med. Chem.* 11:663). The crude solid products were purified by column chromatography using dichloromethane as eluent.

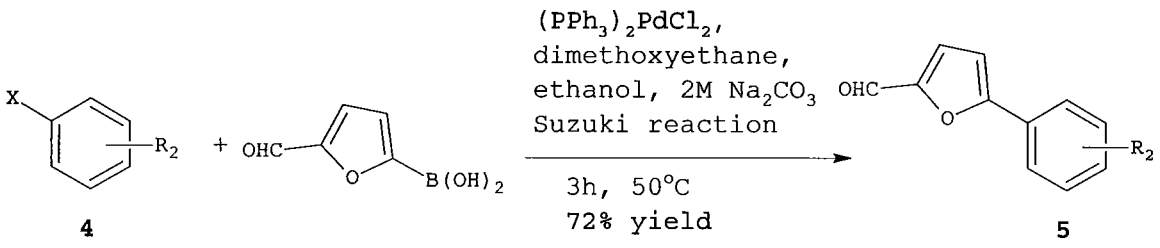

Scheme 3

wherein R_2 is 2-NO_2, 3,4-diMe (**4a**, **5a**); H (**4b**, **5b**); 4-NO_2 (**4c**, **5c**); 2-COOEt (**4d**, **5d**).

*General Procedure for Synthesis of 1-Aryl-3-Methyl-4-[[5-Aryl-2-Furanyl]Methylene]-Pyrazol-5-One (**6**).* The final compounds were synthesized following a modified literature procedure (Scheme 4) (2005) *Russ. J. Org. Chem.* 41:742). An equimolar solution of 1-aryl-3-methyl-pyrazol-5-one, 5-aryl-2-furaldehyde and diethylamine was stirred in ethanol at 50°C for 1-3 hours. On cooling the precipitated red solid was filtered and further purified by column chromatography using 2-10% MeOH/DCM as eluent. The structures of all the compounds were confirmed from 1H NMR, ESI-MS and HRMS analysis.

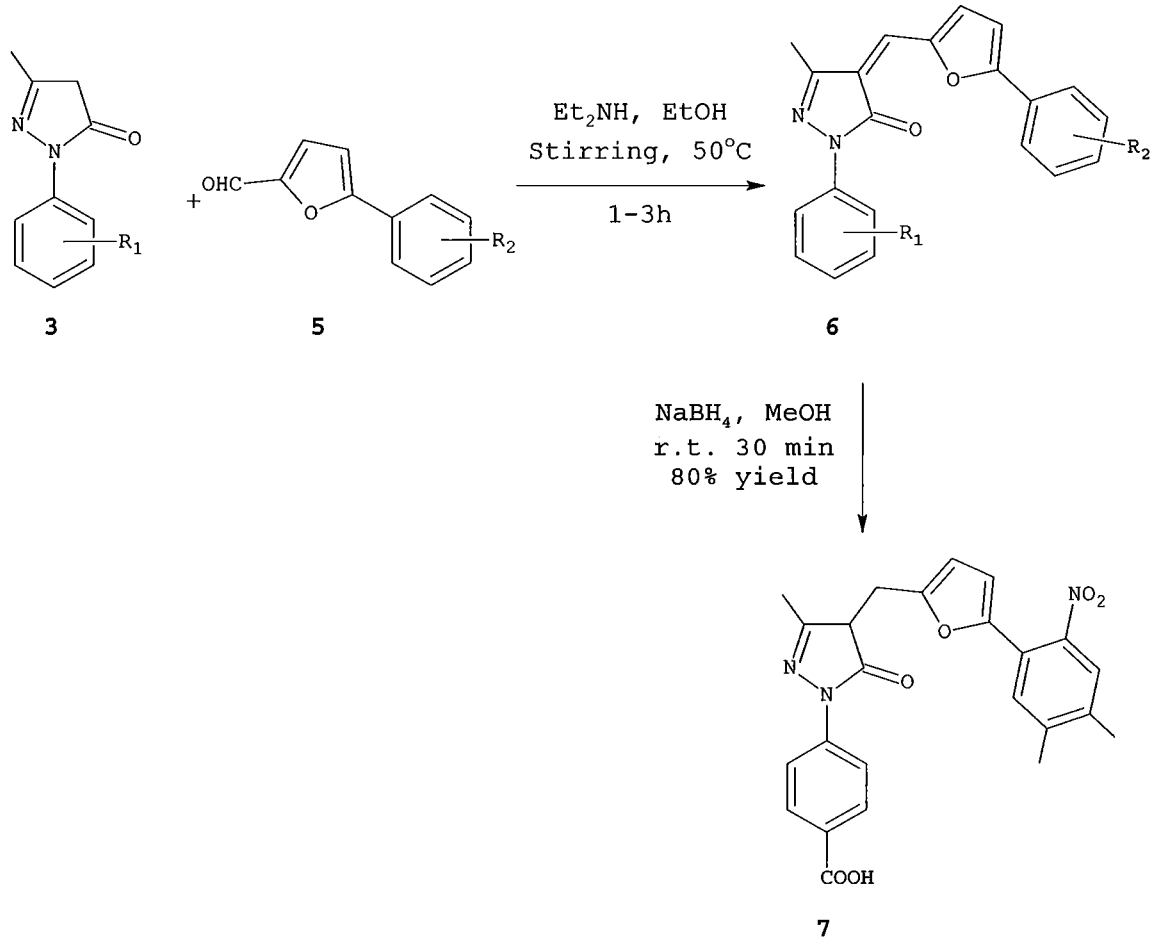

3 5 6 7

Scheme 4

wherein for **3** R_1 is 4-COOH (**3a**), 4-COOEt (**3b**), 4-$CONH_2$ (**3c**), 3-COOH (**3d**), 4-SO_3H (**3e**), 4-Cl (**3f**); for **5** R_2 is 2-NO_2, 3,4-diMe (**5a**), H (**5b**), 4-NO_2 (**5c**), 2-COOEt (**5d**); and for **6a** R_1 is 4-COOH and R_2 is H, **6b** R_1 is 4-COOH and R_2 is 4-NO_2, **6c** R_1 is 4-COOH and R_2 is 2-COOEt, **6d** R_1 is 4-COOEt and R_2 is 2-NO_2, 3,4-diMe, **6e** R_1 is 3-COOH and R_2 is 2-NO_2, 3,4-diMe, **6f** R_1 is 4-SO_3H and R_2 is 2-NO_2, 3,4-diMe, **6g** R_1 is 4-COOH and R_2 is 2-NO_2, 3,4-diMe, **6h** R_1 is 4-$CONH_2$ and R_2 is 2-NO_2, 3,4-diMe, and **6i** R_1 is 4-Cl and R_2 is 2-NO_2, 3,4-diMe.

Compound **6a** was obtained as a red solid in 50% yield, mp 306-309°C. ^1H NMR (400 MHz, DMSO-d_6) δ: 2.35 (3H, s, CH_3), 7.46-7.55 (4H, m, ArH), 7.75 (1H, s, CH), 7.96-8.02 (4H, m, ArH), 8.08 (2H, m, ArH), 8.66 (1H, br s, ArH), 12.84 (1H, br s, COOH); HRMS: Calculated $[M]^+$ for $C_{22}H_{16}N_2O_4$,

372.1110; observed $[M+H]^+$ 373.1189, observed $[M+H]^+$ from ESI-MS: 373.3.

Compound **6b** was obtained as a red solid in 60% yield, mp 338-341°C. ^1H NMR (400 MHz, DMSO-d_6) δ: 2.35 (3H, s, CH_3), 7.73 (2H, d, J = 4.0 Hz, ArH), 7.77 (1H, s, ArH), 7.99 (2H, d, J = 8.8 Hz, ArH), 8.07 (2H, d, J = 8.8 Hz, ArH), 8.17 (2H, d, J = 9.2 Hz, ArH), 8.36 (2H, d, J = 8.8 Hz, ArH), 12.84 (1H, br s, COOH); HRMS: Calculated $[M]^+$ for $C_{22}H_{15}N_3O_6$, 417.0961; observed $[M+H]^+$ 418.1040.

Compound **6c** was obtained as a red solid in 41% yield, mp 249-251°C. ^1H NMR (400 MHz, DMSO-d_6) δ: 1.16 (3H, t, J = 7.6 Hz, $COOCH_2CH_3$), 2.33 (3H, s, CH_3), 4.27 (2H, q, J = 7.0 Hz, $COOCH_2CH_3$), 7.22 (1H, d, J = 4.0 Hz, ArH), 7.60 (1H, d, J = 6.0 Hz, ArH), 7.63 (1H, m, ArH), 7.68-7.81 (2H, m, ArH), 7.87 (1H, d, J = 7.2 Hz, ArH), 8.00-8.02 (2H, m, ArH), 8.08 (2H, d, J = 8.4 Hz, ArH), 8.70 (1H, d, J = 3.2 Hz, ArH), (1H, br s, COOH); HRMS: Calculated $[M]^+$ for $C_{25}H_{20}N_2O_6$, 444.1321; observed $[M+H]^+$ 445.1396, observed $[M+H]^+$ from ESI-MS: 445.2. See WO 2006/129583 and WO 2006/129587.

Compound **6d** was obtained as a red solid in 70% yield, mp 192-194°C. ^1H NMR (400 MHz, $CDCl_3$) δ: 1.40 (3H, t, J = 7.2 Hz, $COOCH_2CH_3$), 2.34 (3H, s, CH_3), 2.38 and 2.39 (6H, 2s, 2 x CH_3), 4.37 (2H, q, J = 7.2 Hz, $COOCH_2CH_3$), 6.92 (1H, d, J = 4.0 Hz, ArH), 7.28 (1H, s, CH), 7.53 (1H, s, ArH), 7.65 (1H, s, ArH), 8.08-8.14 (4H, m, ArH), 8.82 (1H, d, J = 4.0 Hz, ArH); HRMS: Calculated $[M]^+$ for $C_{26}H_{23}N_3O_6$, 473.1587; observed $[M+H]^+$ 474.1660, observed $[M+H]^+$ from ESI-MS: 474.3.

Compound **6e** was obtained as a red solid in 64% yield, mp 260-262°C. ^1H NMR (400 MHz, DMSO-d_6) δ: 2.33, 2.35 and 2.36 (9H, 3s, 3 x CH_3), 7.18 and 7.23 (1H, dd, J = 4.0 and 18.8 Hz, ArH), 7.53-7.58 (2H, m, ArH), 7.70-7.78 (2H, m,

ArH), 7.85 (1H, s, CH), 8.15 (1H, d, J = 7.0 Hz, ArH), 8.55 (1H, d, J = 1.2 Hz, ArH), 8.71 (1H, d, J = 3.2 Hz, ArH), 13.12 (1H, br s, COOH); HRMS: Calculated $[M]^+$ for $C_{24}H_{19}N_3O_6$, 445.1274; observed $[M+H]^+$ 446.1349, observed $[M+H]^+$ from ESI-MS: 446.2.

Compound **6f** was obtained as a red solid in 58% yield, mp 210-213°C. ^1H NMR (400 MHz, DMSO-d_6) δ: 2.31, 2.33 and 2.35 (9H, 3s, 3 x CH_3), 6.90-6.96 (1H, m, ArH), 7.20 (1H, m, ArH), 7.45-7.55 (1H, m, ArH), 7.63-7.72 (2H, m, ArH), 7.76 (1H, s, CH), 7.84 (1H, s, ArH), 7.90 (1H, d, J = 8.4 Hz, ArH), 8.23 (1H, br s, ArH), 10.58 (1H, s, SO_3H); HRMS: Calculated $[M]^+$ for $C_{23}H_{19}N_3O_7S$, 481.0944; observed $[M+H]^+$ 482.1021, observed $[M+H]^+$ from ESI-MS: 482.3.

Compound **6g** was obtained as a red solid in 72% yield. Calculated $[M]^+$ for $C_{24}H_{19}N_3O_6$, 445.1274; observed $[M+H]^+$ from ESI-MS: 446.1. The synthesized **6g** was compared with compound **7** obtained commercially on TLC and found of same R_f (4% MeOH/DCM).

Compound **6h** was obtained as a red solid in 40% yield, mp 273-275°C. ^1H NMR (400 MHz, DMSO-d_6) δ: 2.32, 2.33 and 2.35 (9H, 3s, 3 x CH_3), 7.22 (1H, d, J = 3.2 Hz, ArH), 7.33 (1H, s, ArH), 7.56 (1H, s, ArH), 7.75 (1H, s, 1H), 7.84 (1H, s, ArH), 7.92-8.01 (3H, m, 3ArH, $CONH_2$), 8.68 (1H, d, J = 2.4 Hz, ArH); HRMS: Calculated $[M]^+$ for $C_{24}H_{20}N_4O_5$, 444.1434; observed $[M+H]^+$ 445.1507, observed $[M+H]^+$ from ESI-MS: 445.4.

Compound **6i** was obtained as a red solid in 75% yield, mp 220-223°C. ^1H NMR (400 MHz, $CDCl_3$-d_6) δ: 2.32 (3H, s, CH_3), 2.37 and 2.38 (6H, 2s, 2 x CH_3), 6.90 (1H, d, J = 4.0 Hz, ArH), 7.26 (1H, s, CH), 7.36 (2H, d, J = 8.4 Hz, ArH), 7.51 (1H, s, ArH), 7.63 (1H, s, ArH), 7.94 (2H, d, J = 8.8 Hz, ArH), 8.80 (1H, d, J = 4.0 Hz, ArH); HRMS: Calculated

$[M]^+$ for $C_{23}H_{18}N_3O_4Cl$, 435.0986; observed $[M+H]^+$ 436.1061, observed $[M+H]^+$ from ESI-MS: 436.1.

General Procedure for Synthesis of **7**. To a solution of **6g** (2.24 mmol) in methanol (20 ml), sodium borohydride (2.24 mmol) was added portion-wise, effervescence was evolved and the color of the solution changed from dark red to light yellow. The resulting solution was stirred at room temperature for 30 minutes, solvent was removed and pH of the solution was made 7.0 on adding dilute HCl drop-wise. The resulting mixture was extracted with EtOAc (2 x 50 ml) and concentrated to give an orange solid in 80.0% yield, mp 160-163°C. ^1H NMR (400 MHz, DMSO-d_6) δ: 2.02 (3H, s, CH_3), 2.27 and 2.28 (6H, 2s, 2 x CH_3), 3.56 (2H, s, CH_2), 6.05 (1H, br s, ArH), 6.61 (1H, br s, ArH), 7.50 (1H, s, ArH), 7.61 (1H, s, ArH), 7.85 (2H, d, J = 8.4 Hz, ArH), 8.04 (2H, d, J = 8.4 Hz, ArH), 12.80 (1H, br s, COOH); HRMS: Calculated $[M]^+$ for $C_{24}H_{21}N_3O_6$, 447.1430; observed $[M+H]^+$ 448.1507, observed $[M+H]^+$ from ESI-MS: 448.3.

General Procedure for Synthesis of **9**. 3-Methyl-pyrazol-5-one was synthesized in 60% yield on stirring an equimolar mixture of hydrazine monohydrate and ethyl acetoacetate in ethanol. The exothermic reaction was then cooled in ice-bath to precipitate out a solid white product. The structure of the product was confirmed from ESI-MS and comparing the observed melting point (214-216°C) with the literature melting point (218°C; Singh, et al. (2005) *Eur. J. Pharm. Sci.* 25:255-262). Compound **8** was obtained in on alkylation of 3-methylpyrazol-5-one with equimolar 1-bromovaleric acid by refluxing in 1,4-dioxane for 48 hours following conventional procedures (Belmar, et al. (2005) *J. Braz. Chem. Soc.* 16:179). See Scheme 5. The structure of compound **8** was confirmed from ESI-MS and used for next step without further purification.

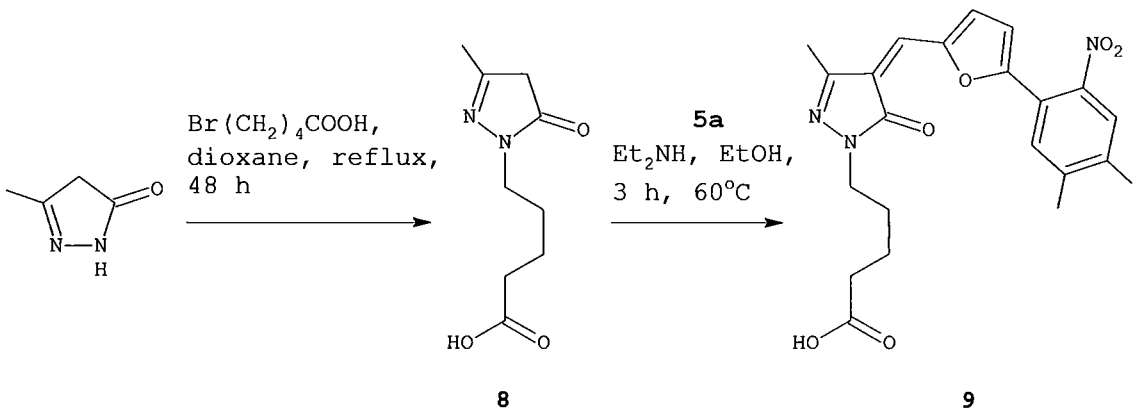

8 9

Scheme 5

Compound **9** was obtained in 15% yield from pyrazole **8** and 5-(2-nitro-4,5-dimethylphenyl)-2-furaldehyde **5a** following the procedure described for the synthesis of compound **6** in Scheme 4. The product was purified by column chromatography using 2-3% MeOH/DCM as eluent. Compound **9** was obtained as a red solid in 15% yield, mp 240-243°C. ^{1}H NMR (400 MHz, $CDCl_3$) δ: 1.58-1.74 (2H, m, CH_2), 2.23 (5H, s and m, CH_3 and CH_2), 2.37 and 2.39 (10H, 2s and 2m, 2 x CH_3 and 2 x CH_2), 6.87 (1H, d, J = 4.0 Hz, ArH), 7.21 (1H, s, CH), 7.52 (1H, s, ArH), 7.63 (1H, s, ArH), 8.71 (1H, br s, COOH), 8.75 (1H, d, J = 4.0 Hz, ArH); HRMS: Calculated $[M]^+$ for $C_{22}H_{23}N_3O_6$, 425.1587; observed $[M+H]^+$ NA.

Example 12: Activity of p300/CBP HAT Inhibitors

Novel HAT inhibitors of the instant invention can be analyzed in a variety of systems with implications for endocrine, cancer, neuropsychiatric, and immunologic therapeutics. The compounds can be assessed in defined well-known model systems used to assess cellular permeability, toxicity, and pharmacodynamic effects. These assays include western blot analysis of histone acetylation as well as HAT-responsive transcriptional reporters that are specific for p300/CBP-mediated acetylation reactions.

Regarding endocrine disorders, it has been found that p300/CBP HAT inhibition by Lys-CoA-Tat blocks CREB signaling and glucagon-induced glucose elevation. These data indicate that novel p300/CBP inhibitors could play a role in the treatment of diabetes mellitus. In addition, it has been shown that Lys-CoA-Tat can inhibit melanoma growth in three different cell lines. New HAT inhibitor scaffolds would thus be useful in treating cancers such as melanoma.

Indeed, the data disclosed herein indicates that inhibitors with a benzoate moiety linked to various aryl groups can inhibit p300/CBP HAT activity (see Tables 1 and 2) and find use in diseases mediated by p300/CBP HAT. Both cell-based assays and animal model studies are performed to further demonstrate efficacy in the treatment of diseases such as cancer.

Cell-Based Assay. Cells from a P388 cell line (CellGate, Inc., Sunnyvale, CA) or human malignant melanoma cell line SK-MEL-2 are grown in RPMI 1640 cell medium containing fetal calf serum (10%), L-glutamine, penicillin, streptomycin and are split twice weekly. All compounds are first diluted with DMSO. Later serial dilutions are done with a phosphate-buffered saline solution. All dilutions are done in glass vials and the final DMSO concentration is generally below 0.5% by volume. Final two-fold dilutions are done in a 96-well plate using cell media so that each well contains 50 μL. All compounds are assayed over multiple concentrations. Cell concentration is measured using a hemacytometer and the final cell concentration is adjusted to about $1X10^4$ cells/mL with cell medium. The resulting solution of cells (50 μL) is then added to each well and the plates are incubated for 5 days in a 37°C, 5% CO_2, humidified incubator. MTT solution (3-[4,5-dimethylthiazol-2-yl]-2,5-diphenyltetrazolium bromide, 10

μL) is then added to each well and the plates are re-incubated under identical conditions for 2 hours. To each well is then added acidified isopropanol (150 μL of i-PrOH solution containing 0.05 N HCl) and mixed thoroughly. The plates are then scanned at 595 nm and the absorbances are read (Wallac Victor 1420 Multilabel Counter). The resulting data is then analyzed to determine an ED_{50} value. Compounds that kill cancer cells, but fail to kill normal cells, find application in the prevention or treatment of cancer.

Mouse Ovarian Carcinoma Zenograft Model. Compounds of the invention are evaluated in an ovarian carcinoma xenograft model of cancer, based on that described by Davis, et al. ((1993) *Cancer Research* 53:2087-2091). This model, in brief, involves inoculating female nu/nu mice with $1X10^9$ OVCAR3-icr cells into the peritoneal cavity. One or more test compounds are administered, *e.g.*, prior to or after tumor cell injection, by the oral route as a suspension in 1% methyl cellulose or intraperitoneally as a suspension in phosphate-buffered saline in 0.01% TWEEN-20. At the conclusion of the experiment (4-5 weeks) the number of peritoneal cells are counted and any solid tumor deposits weighed. In some experiments tumor development is monitored by measurement of tumor specific antigens.

Rat Mammary Carcinoma Model. Compounds of the invention are evaluated in a HOSP.1 rat mammary carcinoma model of cancer (Eccles, et al. (1995) *Cancer Res*. 56:2815-2822). This model involves the intravenous inoculation of $2X10^4$ tumor cells into the jugular vein of female CBH/cbi rats. One or more test compounds are administered, *e.g.*, prior to or after tumor cell injection, by the oral route as a suspension in 1% methyl cellulose or intraperitoneally as a suspension in phosphate-buffered saline and 0.01% TWEEN-20. At the conclusion of the experiment (4-5 weeks)

the animals are killed, the lungs are removed and individual tumors counted after 20 hours fixation in Methacarn.

Mouse B16 Melanoma Model. The anti-metastatic potential of compounds of the invention is evaluated in a B16 melanoma model in C57BL/6. Mice are injected intravenously with $2X10^5$ B16/F10 murine tumor cells harvested from *in vitro* cultures. Inhibitors are administered by the oral route as a suspension in 1% methyl cellulose or intraperitoneally as a suspension in phosphate-buffered saline pH 7.2 and 0.01% TWEEN-20. Mice are killed 14 days after cell inoculation and the lungs removed and weighed prior to fixing in Bouin's solution. The number of colonies present on the surface of each set of lungs is then counted.

What is claimed is:

1. A method for identifying a compound which modulates the activity of p300/CBP comprising

(a) designing or screening for a compound which binds to at least one amino acid residue of the lysine-CoA inhibitor binding site, L1 loop, electronegative pocket, or electronegative groove of the histone acetyltransferase (HAT) domain of p300/CBP; and

(b) testing the compound designed or screened for in (a) for its ability to modulate the activity of p300/CBP, thereby identifying a compound that modulates the activity of p300/CBP.

2. The method of claim 1, wherein the compound binds to the substrate binding site and inhibits the activity of p300/CBP.

3. The method of claim 1, wherein step (a) is carried out *in silico*.

4. The method of claim 1, wherein step (a) is carried out *in vitro*.

5. A compound identified by the method of claim 1.

6. A pharmaceutical composition comprising a compound identified by the method of claim 1 in admixture with a pharmaceutically acceptable carrier.

7. A p300/CBP inhibitor selected from the group set forth in Table 2.

8. A pharmaceutical composition comprising a p300/CBP inhibitor of claim 7 in admixture with a pharmaceutically acceptable carrier.

9. A method for making an inhibitor of p300/CBP comprising screening for a compound which interacts with amino acid residues Arg1410, Thr1411, Trp1466, and Tyr1467 of SEQ ID NO:1 or amino acid residues Arg1446, Thr1447, Trp1502 and Tyr1503 of SEQ ID NO:2 thereby making an inhibitor of p300/CBP.

10. A method for modulating the activity of p300/CBP comprising contacting a p300/CBP protein with a compound of claim 5 thereby modulating the activity of p300/CBP.

11. A method for preventing or treating cancer, obesity, or diabetes comprising administering to a subject in need of treatment the pharmaceutical composition of claim 6, thereby preventing or treating cancer, obesity, or diabetes in the subject.

12. A method for preventing or treating cancer, obesity, or diabetes comprising administering to a subject in need of treatment the pharmaceutical composition of claim 8, thereby preventing or treating cancer, obesity, or diabetes in the subject.

13. A method for producing a heterodimeric histone acetyltransferase (HAT) complex comprising

subjecting a HAT domain and N-Cys peptide of p300/CBP to expressed protein ligation to produce a semi-synthetic HAT domain; and

subjecting the semi-synthetic HAT domain to proteolysis in the presence of an inhibitor thereby producing a heterodimeric HAT complex.

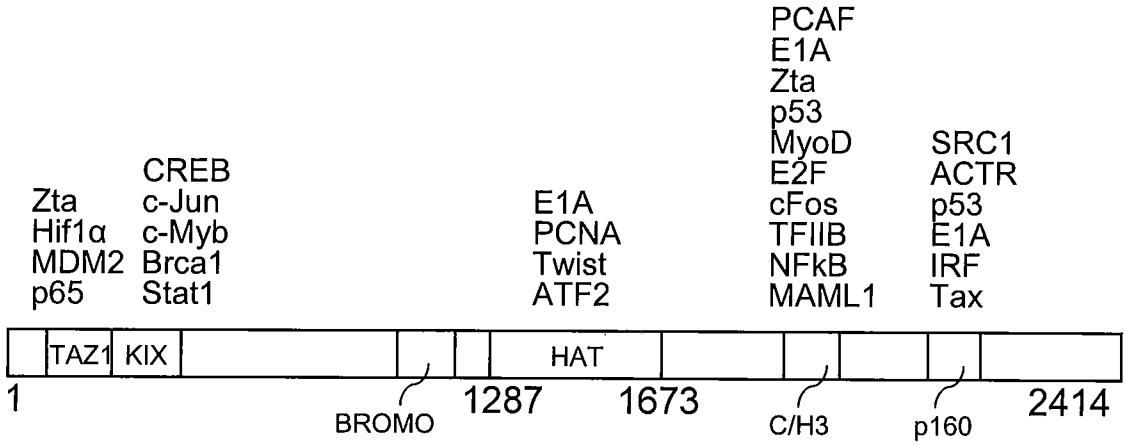
PCAF
E1A
Zta
p53
MyoD
E2F
cFos
TFIIB
NFkB
MAML1
SRC1
ACTR
p53
E1A
IRF
Tax
CREB
c-Jun
c-Myb
Brca1
Stat1
Zta
Hif1α
MDM2
p65
E1A
PCNA
Twist
ATF2
TAZ1
KIX
HAT
1
BROMO
1287
1673
C/H3
p160
2414

FIG. 1A

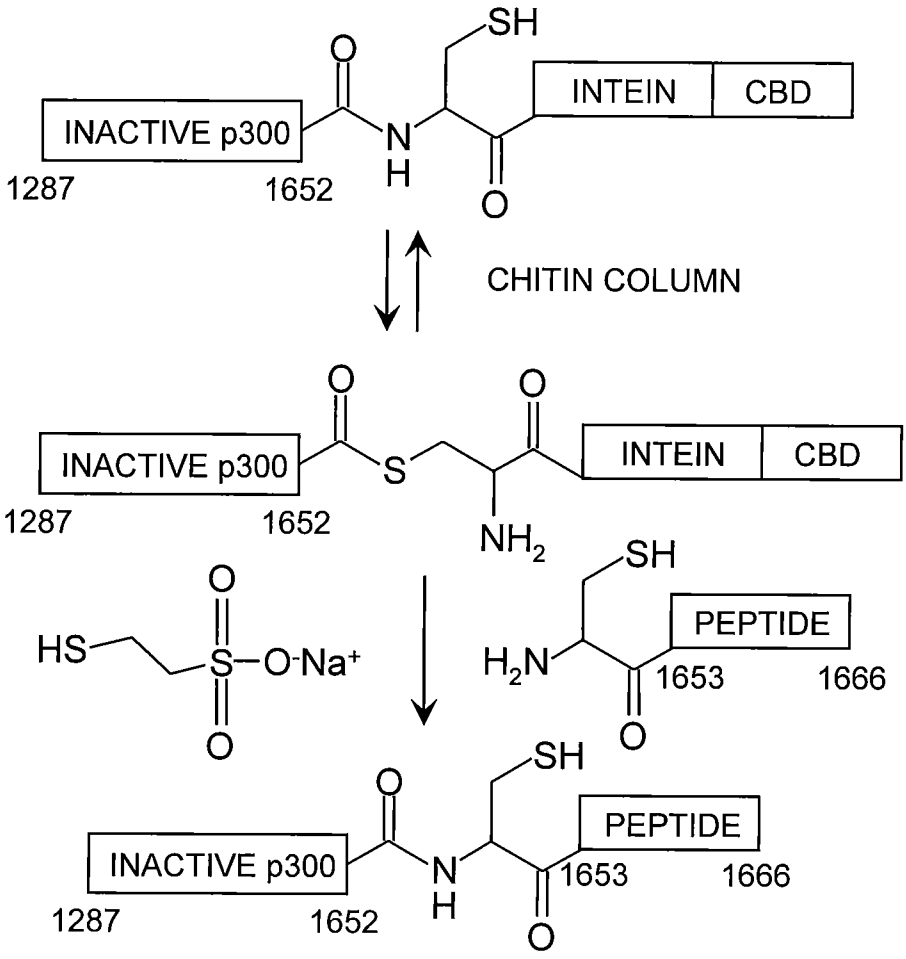
SH
O
INACTIVE p300
N
H
INTEIN
CBD
1287
1652
O
CHITIN COLUMN
O
O
INACTIVE p300
S
INTEIN
CBD
1287
1652
NH2
SH
O
HS
S
O-Na+
PEPTIDE
H2N
1653
1666
O
O
SH
O
PEPTIDE
INACTIVE p300
N
H
1653
1666
1287
1652
O

FIG. 1B

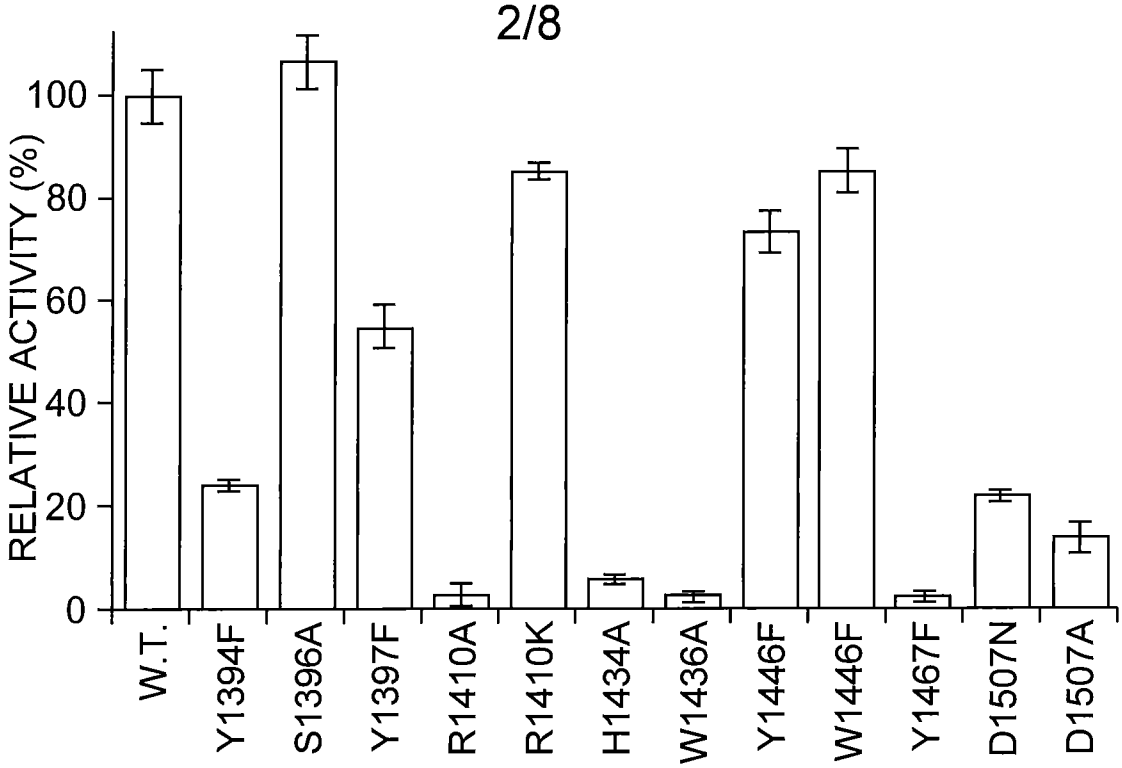
RELATIVE ACTIVITY (%)
100
80
60
40
20
0
W.T.
Y1394F
S1396A
Y1397F
R1410A
R1410K
H1434A
W1436A
Y1446F
W1446F
Y1467F
D1507N
D1507A

FIG. 2

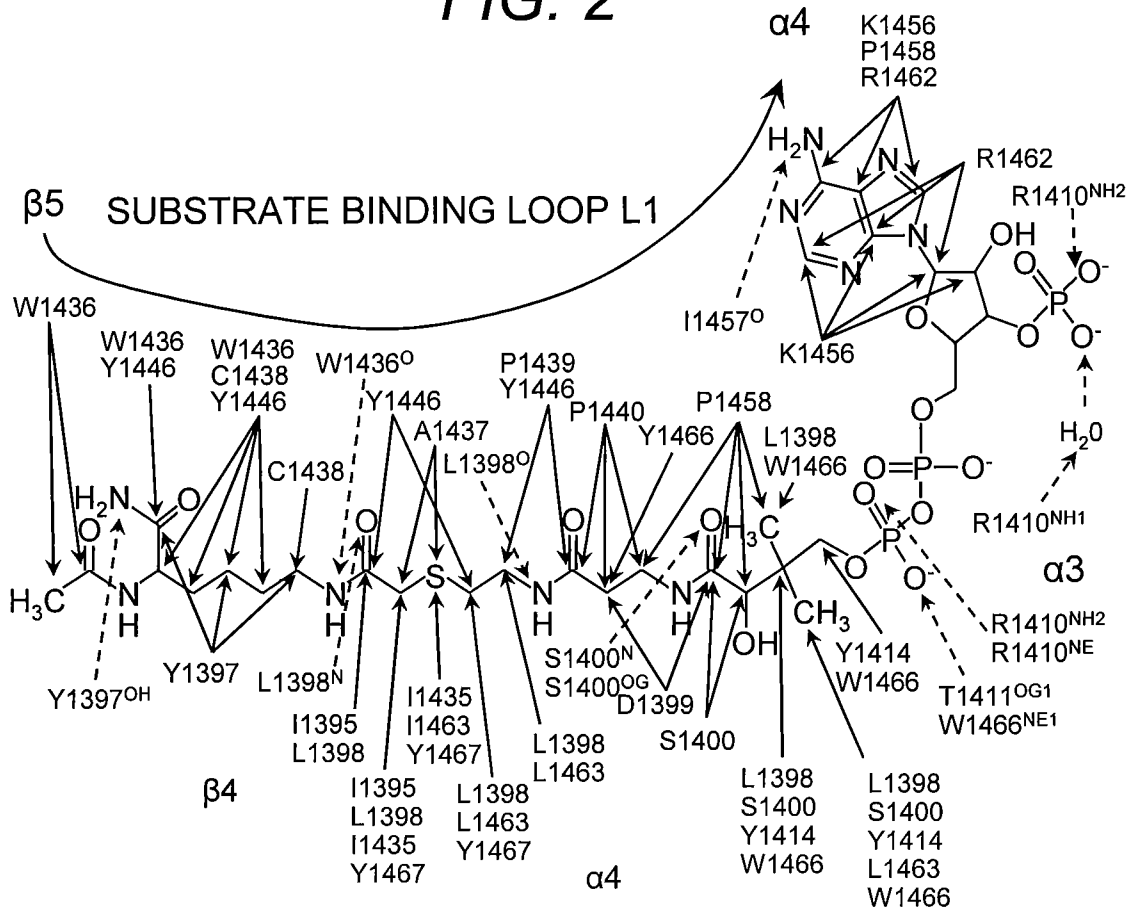
α4
K1456
P1458
R1462
β5
SUBSTRATE BINDING LOOP L1
R1462
R1410NH2
I1457O
K1456
W1436
W1436
Y1446
W1436
C1438
Y1446
W1436O
Y1446
P1439
Y1446
A1437
L1398O
P1440
Y1466
P1458
L1398
W1466
C1438
H2O
R1410NH1
α3
Y1397OH
Y1397
L1398N
I1395
L1398
I1435
I1463
Y1467
S1400N
S1400OG
D1399
S1400
Y1414
W1466
T1411OG1
W1466NE1
R1410NH2
R1410NE
β4
I1395
L1398
I1435
Y1467
L1398
L1463
Y1467
L1398
L1463
L1398
S1400
Y1414
W1466
L1398
S1400
Y1414
L1463
W1466
α4

FIG. 3

```
  1 - S G R G K Q G G K A R A K A K S R S S   H2A
  8 - P A P K K G S K K A V T K A Q K K D G   H2B
 10 - S T G G K A P R K Q L A T K A A R K S   H3
  4 - G K G G K G L G K G G A K R H R K V L   H4

364 - A H S S H L K S K K G Q S T S R H K K   p53
322 - N G A A S K R A F K Q S P P A V P A L   p73
 49 - V Q T K G K R G A K G K Q A E Y A Y Q   HMG14
111 - R G R H P G K G V K S P G E K S R Y E   E2F1
 16 - C S T D E V K I F K D E G D R E D E K   dTCF
 59 - R P R G R P K G S K N K G A A K T R K   HMGI(Y)
348 - N E D P D E K R R K F L E R N R A A A   ATF-2
481 - A Q E I K Y G P L K M L P Q T P S H L   c-Myb
301 - K R K R T Y E T F K S I M K K S P F S   NFKB
676 - D I P K E E A F G K Y C R P E S Q E H   STAT3
303 - Q T R N R K A S G K G K K K R G S N L   mGATA-1
 90 - A G R C L L W A C K A C K R K T T N A   MyoD
621 - E A G M T L G A R K L K K L G N L K L   AR
 41 - K A L G I S Y G R K K R R Q R R R A H   Tat
1542 - K G D S K N A K K K N N K K T S K N K   p300
```

FIG. 4

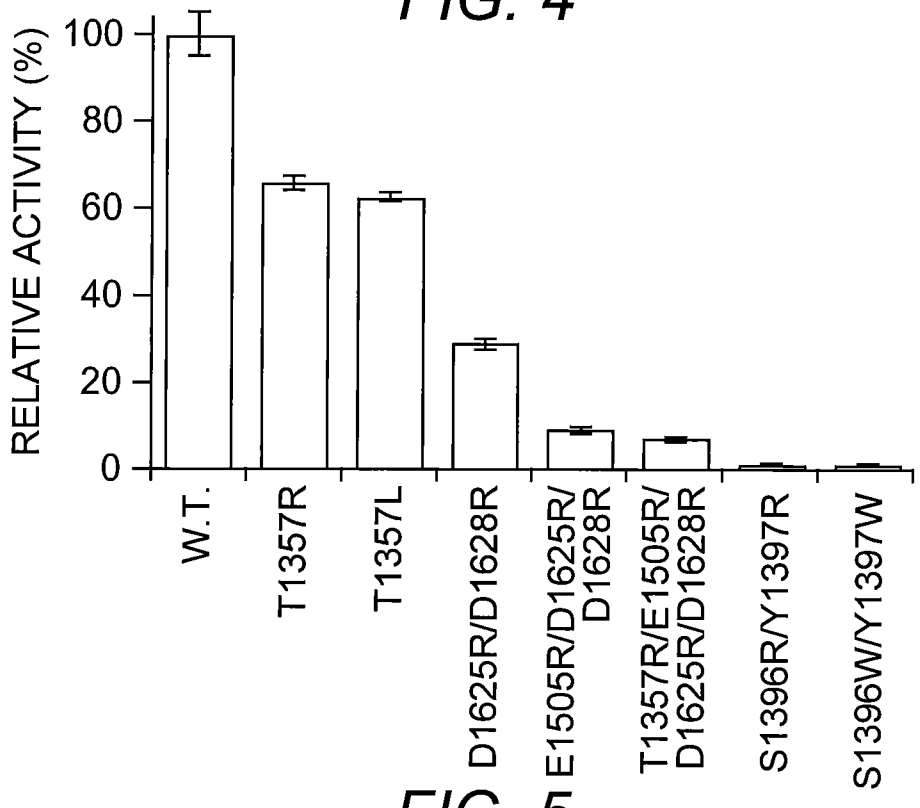

FIG. 5

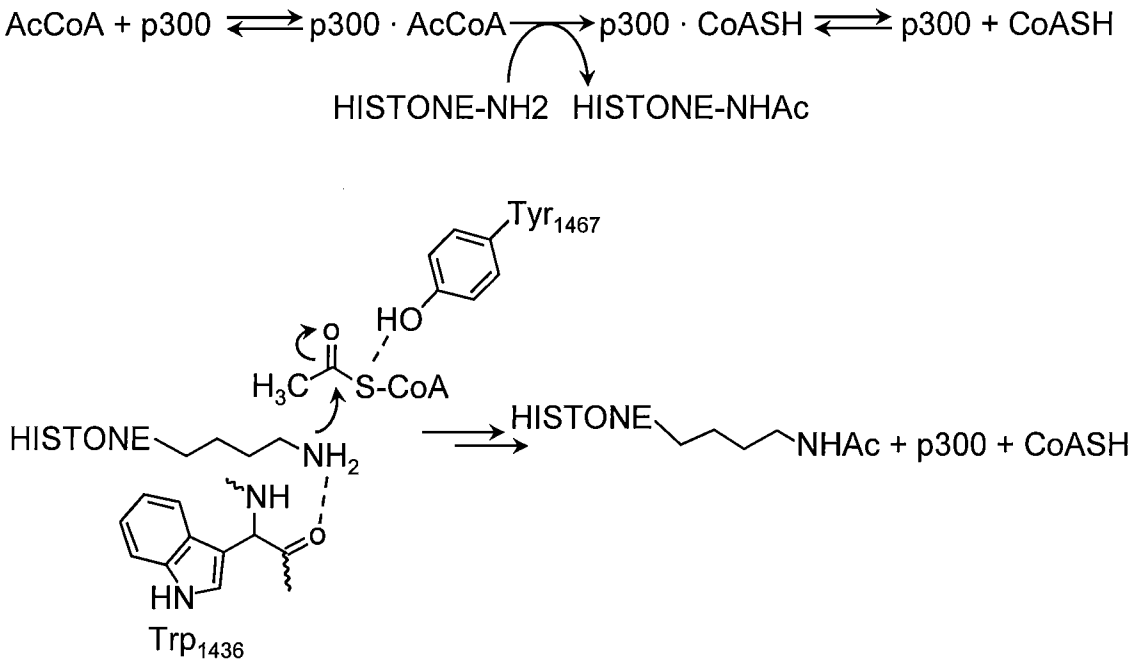
AcCoA + p300
p300 · AcCoA
p300 · CoASH
p300 + CoASH
HISTONE-NH2
HISTONE-NHAc
Tyr1467
HO
O
H3C
S-CoA
HISTONE
NH2
NH
O
HN
Trp1436
HISTONE
NHAc + p300 + CoASH

FIG. 6A

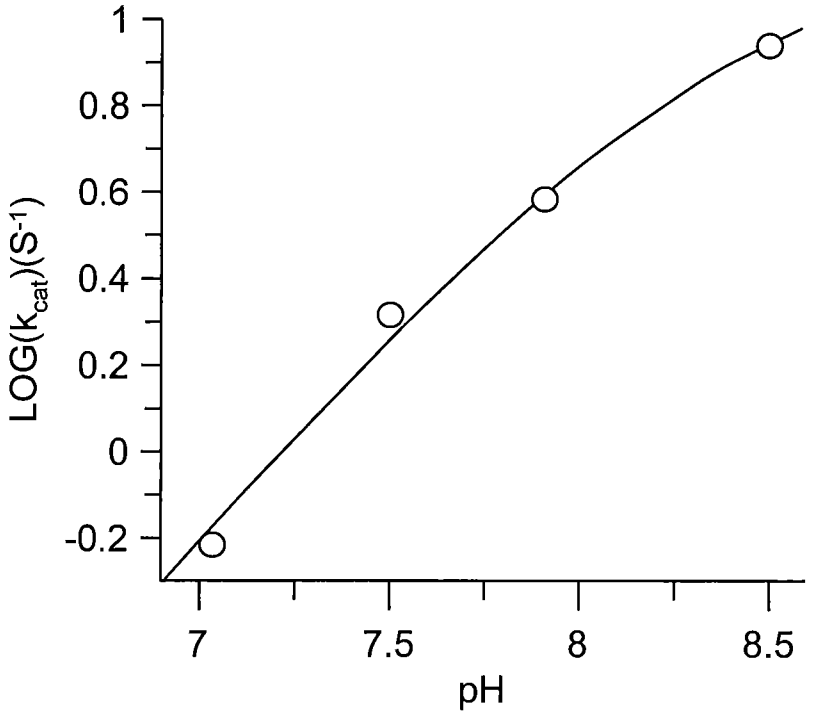
1
0.8
0.6
0.4
0.2
0
-0.2
LOG(kcat)(S-1)
7
7.5
8
8.5
pH

FIG. 6B

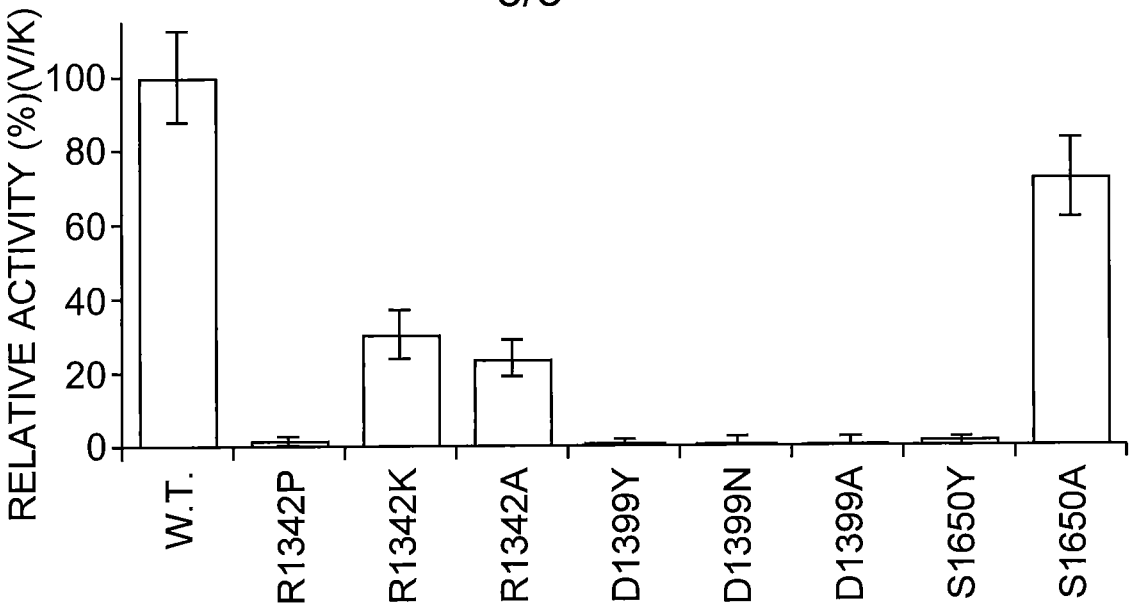
RELATIVE ACTIVITY (%)(V/K)
100
80
60
40
20
0
W.T.
R1342P
R1342K
R1342A
D1399Y
D1399N
D1399A
S1650Y
S1650A

FIG. 7

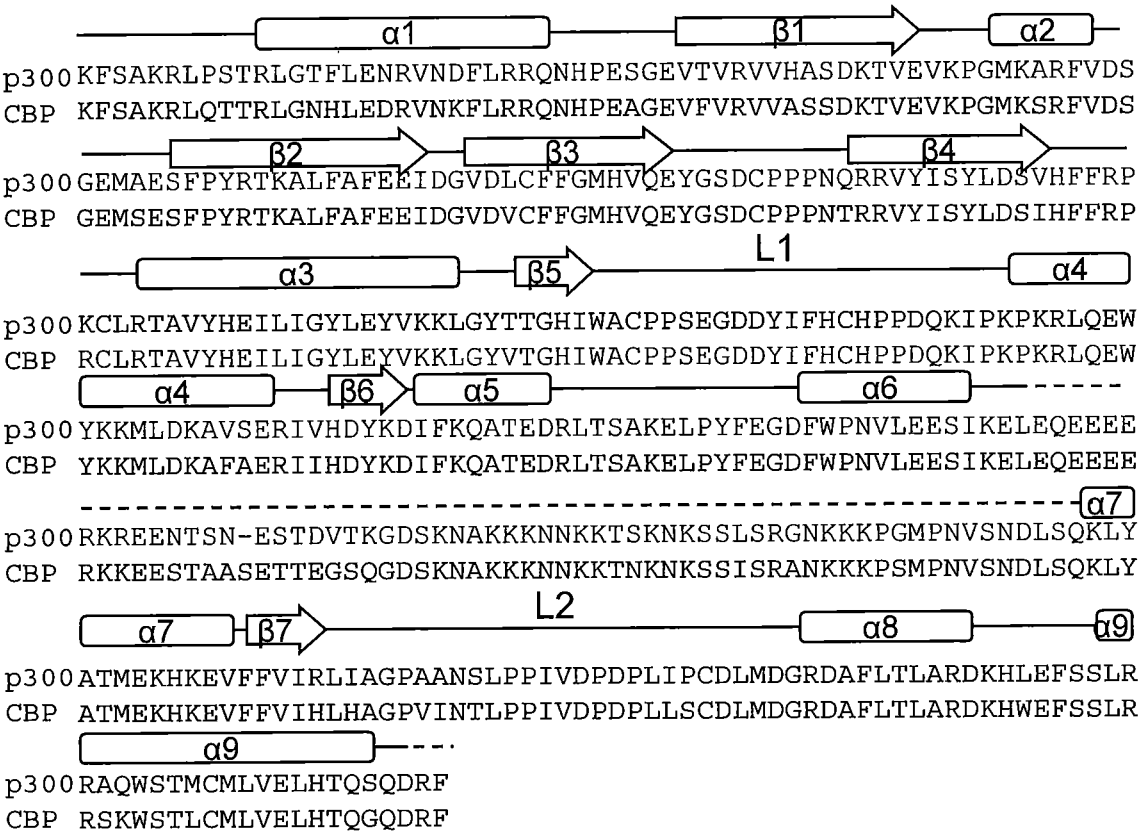
α1
β1
α2
p300 KFSAKRLPSTRLGTFLENRVNDFLRRQNHPESGEVTVRVVHASDKTVEVKPGMKARFVDS
CBP KFSAKRLQTTRLGNHLEDRVNKFLRRQNHPEAGEVFVRVVASSDKTVEVKPGMKSRFVDS
β2
β3
β4
p300 GEMAESFPYRTKALFAFEEIDGVDLCFFGMHVQEYGSDCPPPNQRRVYISYLDSVHFFRP
CBP GEMSESFPYRTKALFAFEEIDGVDVCFFGMHVQEYGSDCPPPNTRRVYISYLDSIHFFRP
L1
α3
β5
α4
p300 KCLRTAVYHEILIGYLEYVKKLGYTTGHIWACPPSEGDDYIFHCHPPDQKIPKPKRLQEW
CBP RCLRTAVYHEILIGYLEYVKKLGYVTGHIWACPPSEGDDYIFHCHPPDQKIPKPKRLQEW
α4
β6
α5
α6
p300 YKKMLDKAVSERIVHDYKDIFKQATEDRLTSAKELPYFEGDFWPNVLEESIKELEQEEEE
CBP YKKMLDKAFAERIIHDYKDIFKQATEDRLTSAKELPYFEGDFWPNVLEESIKELEQEEEE
α7
p300 RKREENTSN-ESTDVTKGDSKNAKKKNNKKTSKNKSSLSRGNKKKPGMPNVSNDLSQKLY
CBP RKKEESTAASETTEGSQGDSKNAKKKNNKKTNKNKSSISRANKKKPSMPNVSNDLSQKLY
L2
α7
β7
α8
α9
p300 ATMEKHKEVFFVIRLIAGPAANSLPPIVDPDPLIPCDLMDGRDAFLTLARDKHLEFSSLR
CBP ATMEKHKEVFFVIHLHAGPVINTLPPIVDPDPLLSCDLMDGRDAFLTLARDKHWEFSSLR
α9
p300 RAQWSTMCMLVELHTQSQDRF
CBP RSKWSTLCMLVELHTQGQDRF

FIG. 8A

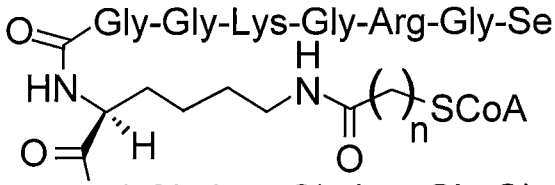

H4-CoA-20-L

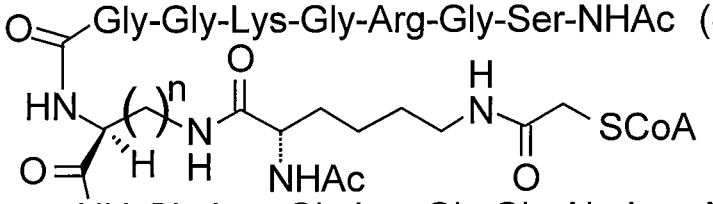

H4-CoA-20-X

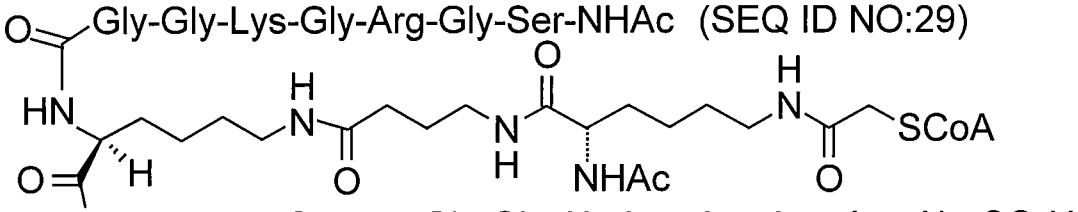

H4-CoA-20-Z

FIG. 9

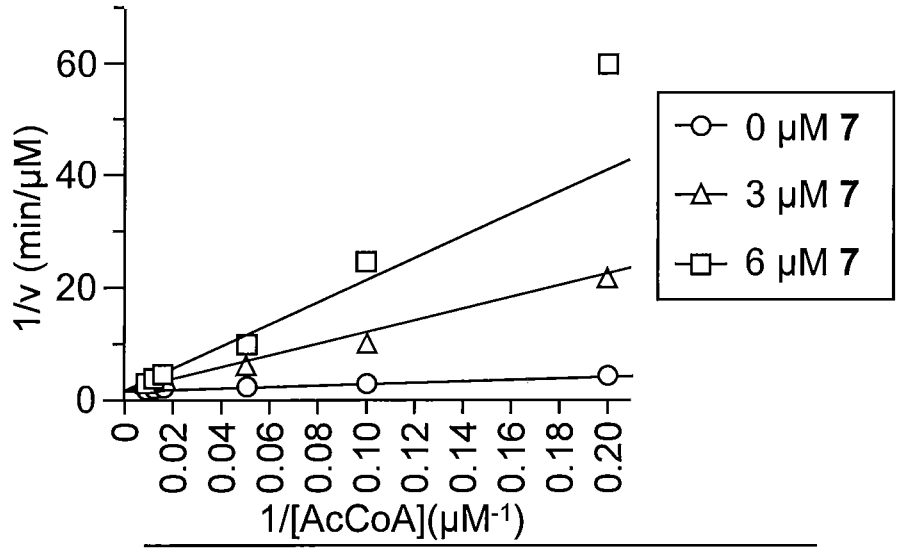

PARAMETER	VALUE	STD. ERROR
Vmax (μM/min)	0.6956	0.0258
Km (μM)	8.5082	1.3691
Ki (μM)	0.3989	0.0612

FIG. 10A

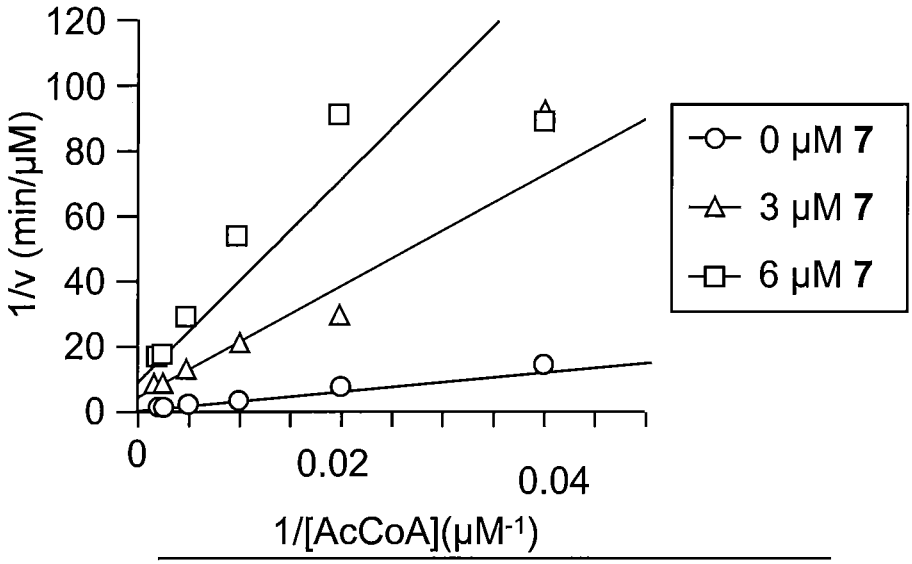

PARAMETER	VALUE	STD. ERROR
Vmax (μM/min)	0.8791	0.0279
Km (μM)	255.5391	17.7592
Ki (μM)	0.6145	0.1274
Ki' VALUE (μM)	0.9317	0.2098

FIG. 10B

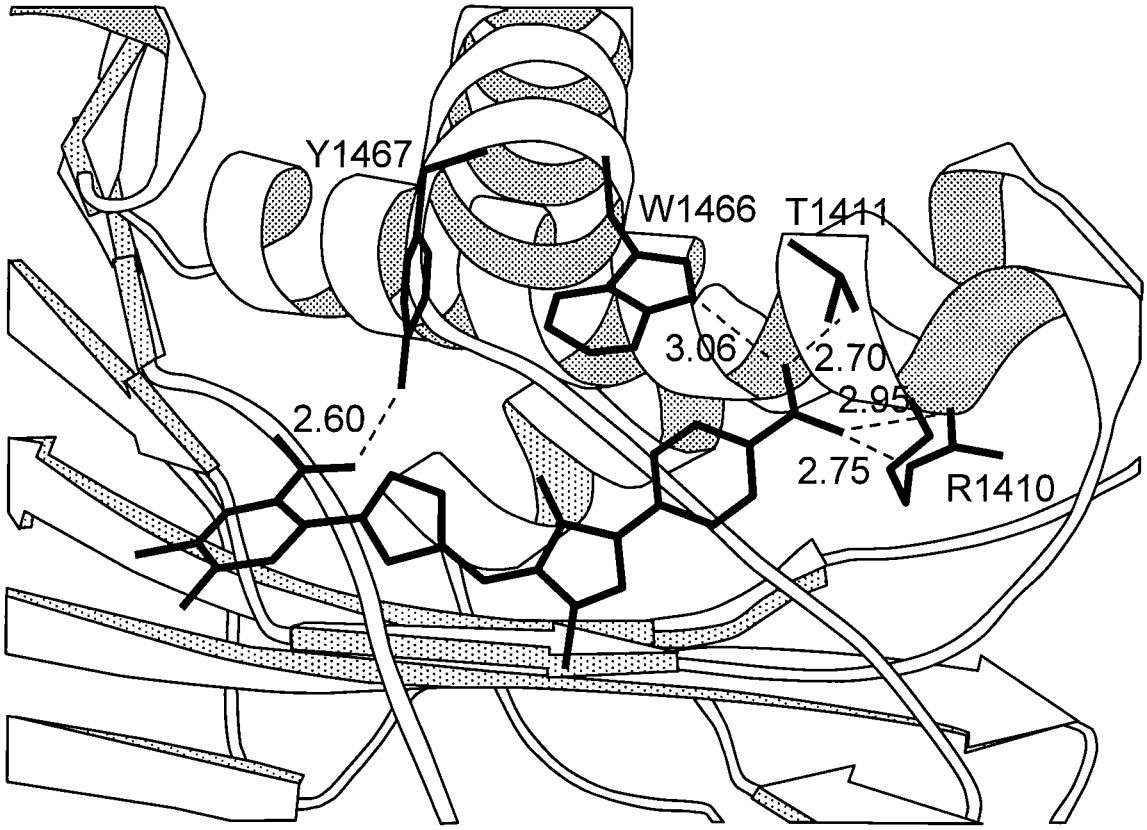

FIG. 11